Decadal Evaluation of the AIRPACT Regional Air Quality Forecast System in the Pacific Northwest from 2009-2018

Jordan A. Munson[1#], Joe Vaughan[1], Brian Lamb[1], and Yunha Lee[1*]

[1]Laboratory for Atmospheric Research Civil and Environmental Engineering, Washington State University, Pullman, 99163, United States

[#]now at Wisconsin Department of Natural Resources, Madison, WI 53707-7921
[*]now at Center for Advanced Systems Understanding, Helmholtz-Zentrum Dresden–Rossendorf, Dresden, Germany

Correspondence to: Yunha Lee (y.lee@hzdr.de)

Abstract. The Air Indicator Report for Public Awareness and Community Tracking (AIRPACT) is a comprehensive, automated air quality forecast system that provides 48-hr in-advance air quality over the Pacific Northwest region (http://lar.wsu.edu/airpact/). Since 2001, the AIRPACT forecasting system has been successfully operated by Washington State University, with the financial support from the Northwest International Air Quality and Environmental Science consortium (NW-AIRQUEST). AIRPACT consists of the Sparse Matrix Operator Kernel Emissions (SMOKE) model to provide temporal and spatial emissions, the Community Multiscale Air Quality (CMAQ) model to simulate hourly ozone, particulate matter and related precursor concentrations over the Pacific Northwest region, and the Weather Research and Forecasting (WRF) model to simulate meteorology fields which are inputs for CMAQ: WRF is run by University of Washington and their outputs are transferred to Washington State University. AIRPACT is one of the longest operational regional air quality forecast system in the US that is based on a chemical transport modeling. In this paper, we have evaluated AIRPACT forecasts for the last ten years (2009-2018) against quality-controlled EPA Air Quality System observations, with particular focus on examining how overall air quality forecast skill has changed as the AIRPACT system has evolved. During this period, AIRPACT has been intermittently updated with improved physical and chemical processes as well as newer emissions and higher resolution model domains. Our evaluation results show that AIRPACT's skill at forecasting ozone (O_3) has improved over time. However, the fine particulate matter ($PM_{2.5}$), forecast performance has decreased over time.

This is a non peer-reviewed preprint submitted to EarthArxiv.

The $PM_{2.5}$ forecasts in the most recent version of AIRPACT were underpredicted to a larger degree than the previous version, partly because elevated $PM_{2.5}$ concentrations during the wildfire season in the years 2015 and 2018 were underestimated. In order to improve overall air quality forecast accuracy, our future efforts should focus on building a more reliable forecast system to handle extreme air quality events in combination with using new techniques for data-assimilation, ensemble forecasting, and statistical post-processing.

1 Introduction

Ambient air pollution is responsible for almost 3 million deaths each year globally, making it a major concern for public health (WHO, 2016). In recent years, air pollution has received public attention, as many cities, particularly in developing countries, experienced dangerous levels of air pollution that caused a serious health burden. In the US, air pollution has greatly improved over time due to the Clean Air Act (CAA) implemented by the U.S. Environmental Protection Agency (U.S. EPA) (U.S. EPA, 2015a). Regulatory policy has been controlling outdoor air pollution effectively; however, it is not realistic to eliminate air pollution entirely, and pollutants are transported in the ambient air for days or weeks (depending on the species), which makes air pollution a global problem. Some pollutants can be harmful even at ambient concentrations, especially for sensitive groups such as children (Neidell, 2004). Therefore, to protect public health from outdoor air pollution more effectively, a proactive action, such as advising a sensitive population group about upcoming air quality information, might be necessary.

Ozone and particulate matter with a diameter less than 2.5 µm ($PM_{2.5}$), are criteria pollutants that are regulated under the CAA as their adverse health impact on the public. According to Fann et al. (2012), $PM_{2.5}$ pollution was responsible for 130,000 deaths in 2005 within the U.S. and ozone pollution for 4,700 deaths. Informing the public with ozone and particulate matter forecasts would be a proactive step towards preventing sickness and death related to air pollution.

Since 2001, the Laboratory for Atmospheric Research at Washington State University has operated the AIRPACT (Air Indicator Report for Public Awareness and Community Tracking) air quality forecast system successfully for Pacific Northwest (PNW)(Mass et al., 2003; Vaughan et al., 2004; Mahmud, 2005; Chen, et al., 2008). Currently, the modeling components in AIRPACT include the WRF (Weather Research and Forecasting) meteorology model, SMOKE (Sparse Matrix Operator Kernel for Emissions) emission processing tool, and CMAQ (Community Multiscale Air Quality) chemical transport model along with chemical boundary conditions provided via the NCAR Whole Atmosphere Community Climate Model (WACCM; https://www.acom.ucar.edu/waccm/forecast/): WRF-based meteorology forecasts have been operated by Prof. Cliff Mass at University of Washington and delivered to Washington State University daily. NW-AIRQUEST (Northwest International Air Quality and Environmental Science consortium) has provided financial support to AIRPACT with the goal of protecting human health and other values by protecting air quality. NW-AIRQUEST is a group including federal, state, local and tribal air quality agencies (e.g., US EPA Region 10, the WA Department of Ecology, the Oregon Department of Environmental Quality and the Idaho Department of Environmental Quality, and the Puget Sound Clean Air Agency, among others).

AIRPACT predicts several air pollutants including surface ozone and PM2.5 to 1) assist state and local air quality managements to make short-term and long-term plans to improve air quality in their jurisdictions and 2) forewarn the public, especially during the extreme air pollution events such as wildfires, so that they can make informed decisions on their activities. Along with the surface air pollution levels, AIRPACT also reports hourly air pollutant emissions, chemical boundary conditions used in AIRPACT, and observations in handy visualizations to enable the public to understand the information easily. All our AIRPACT products are freely available via our website (http://lar.wsu.edu/airpact/).

The PNW region experiences various air quality events including stratospheric ozone intrusions, primarily in spring, prescribed agricultural burning in spring and fall, wildfires in summer and fall, and residential wood burning in winter. Wildfire smoke causes notoriously poor AQ during summers in the region. The PNW region is also influenced by long-range transport of air pollutants from Asia (Jaffe et al., 1999). Extreme air pollution events such as stratospheric ozone intrusion and wildfires makes air quality forecasting challenging. As AIRPACT is based a 3-D gridded air quality model, our forecasts are also subject to uncertainties in input datasets (e.g., emissions, chemical boundary conditions and meteorology) and from parameterizations of sub-grid scale and complex physical and chemical processes. Thus, our group has constantly evaluated our forecasts against observations and have modified AIRPACT system to provide more accurate forecasts to the public. As a routine process, AIRPACT is evaluated daily against AIRNOW (pre-quality-control) observations, and performance statistics are published online. AIRPACT underwent more thorough evaluations against the surface observation networks and satellite products;

for example, Chen et al. (2008) evaluated the AIRPACT version 3 against EPA's Air Quality System observations (AQS), IMPROVES and SWACCA during August-November 2004; Herron-Thorpe et al. (2010) evaluated the tropospheric NO2 column of AIRPACT version 3 against the OMI/Aura satellite NO2 products from March 2007 to August 2008; and Herron-Thorpe et al. (2014) performed a comprehensive evaluation of AIRPACT version 3 for the 2007 and 2008 wildfire season using a suite of surface and satellite observations (i.e., EPA's AQS, AQUA-MODIS aerosol optical depth, OMI tropospheric NO_2, AIRS CO, and CALIOP aerosols). However, there has not been a long term, multi-year evaluation study using AIRPACT.

In this paper, we have evaluated AIRPACT ozone and $PM_{2.5}$ forecasts from the last 10 years (2009 to 2018) against the EPA's AQS observations, with a primary focus on how the AIRPACT forecast skill has progressed as our modeling system went through the major updates. Our archived data is limited to hourly ozone and $PM_{2.5}$ and basic meteorology data at EPA AQS sites, because we were not able to save all AIRPACT forecast products due to data storage costs; each day of forecast data takes many gigabytes of space. The meteorology evaluation is provided in the supplementary materials as the evaluation is limited because of large gaps in meteorological output during 2009-2012.

During the 2009-2018 period, AIRPACT underwent two major updates: from version 3 (hereafter, AP-3) to version 4 (hereafter, AP-4) and to version 5 (hereafter, AP-5). Table 1 provides a summary of each AIRPACT version. Note that we provide only model version number for WRF, CMAQ, and SMOKE. Please refer the details of updates made to each model in the relevant developer group, using the version number. Given that each major AIRPACT update involved many minor updates and we have not maintained access to older AIRPACT models, our analysis is mainly focused on describing the changes in forecast skills among the AIRPACT versions and, when possible, we provide a potential cause for such changes.

2 The AIRPACT Air Quality Forecast System

Our AIRPACT system simulates hourly O_3 and PM2.5 and related precursor levels over the PNW region, and consists of WRF, SMOKE, and CMAQ. The WRF forecasts used in AIRPACT are generated daily by the University of Washington (UW); the specific details of the WRF model setup are available at this website (https://atmos.washington.edu/wrfrt/info.html). With the completion of the WRF forecast at the UW, the MCIP (Meteorology-Chemistry Interface Processor) preprocessor is run to extract WRF output fields for transfer to WSU, where the MCIP meteorology files are used as input both for SMOKE emissions processing and for CMAQ chemical transport model, which results in the AQ forecast. As supplementary information, we have provided the list of publications related to AIRPACT from Laboratory for Atmospheric Research, Washington State University.

The current version, AP-5, uses SMOKE v3.5.1, CMAQ v5.0.2, and WRF v3.7.1 over a domain that includes the entirety of Washington, Oregon, and Idaho and the adjoining parts of Canada, western Montana, and small northern sections of California, Nevada, and Utah. The AP-5 modeling system is depicted in S-Fig. 1. The model horizontal grid spans 285 columns west to east, spans 258 rows south to north, with grid cells of 4 km x 4 km and with 37 vertical layers, the lowest of which is ~40 meters deep. The AP-4 system used CMAQ v4.7.1, SMOKE v2.7 and v3.5, and WRF v3.4.1 and v3.5. AP-4 used the same domain and horizontal grid as AP-5, but with only 21 vertical layers. The AP-3 system used CMAQ v4.6, SMOKE v2.1, and WRF v3.1.1 with 12 km x 12 km grid cells and 21 vertical layers. AP-3 had a slightly larger domain that extended further north (see S-Fig. 2). The number of vertical layers in AP-5 was changed from 21 layers to 37 layers in order to better resolve the tropopause and to better capture stratospheric ozone intrusion events. Note that the WRF meteorology from UW provided 37 vertical layers for AP-3 and AP-4, but layer collapsing in MCIP had condensed those to 21 layers for AIRPACT to control CMAQ computing time.

Throughout the last three versions of AIRPACT, the CMAQ model has been updated with an available newer version (see Table 1). One of the significant updates occurred in AP-5, which uses 1) CMAQ 5.0.2 that has an improvement in particulate matter (PM) speciation (i.e., separated the old term "PM_{other}" into 12 more PM categories) and 2) the carbon bond gas-phase mechanism (CB05) instead of SAPRC99. The latter change was based on the two main findings from Luechen et al. (2008): CB05 is faster than SAPRC99, which helps to reduce CMAQ computing time, and it tends to predict lower ozone concentrations than SAPRC99 on average. AIRPACT with SAPRC99 tended to overpredict ozone values, so the switch to CB05 was in part an attempt to reduce ozone overprediction.

The AIRPACT system includes a comprehensive set of emissions, including mobile, non-mobile, biogenic and fire sources, that account for spatial and temporal variation (see the details in Table 1). Different emissions types and inputs are combined and assigned to grid cells using SMOKE. To handle mobile emissions, AIRPACT used the MOBILE6 model in AP-3 and in AP-4 but switched partway through AP-4 to MOVES. MOVES was developed in response to concerns from the National Research Council that the MOBILE6 model was insufficient and was designed to be more adaptive and easier to use (Koupal, Cumberworth, Michaels, Beardsley, & Brzezinski, 2003); the EPA no longer uses MOBILE6 and no longer accepts the use of that model for regulatory analysis. MOVES emissions are based on modes, which is a method within MOVES to characterize local emissions on a finer scale than the MOBILE6 vehicle emissions which are based solely on a regional patterns. Thus these modes in MOVES allow a finer definition of emissions (Beardsley, Warila, Dolce, & Koupal, 2009). MOVES is the currently maintained model and gets updated with newer emissions and activity data (U.S. EPA, 2016a).

Non-mobile emissions for AIRPACT are gathered from state emissions inventory reports and the National Emissions Inventory (NEI). The NEI is a product produced by the EPA that contains an estimate of criteria air pollutant emissions; a new NEI version is released every three years (U.S. EPA, 2015b). To maintain emissions up-to-date, the NEI inventory used in AIRPACT has been updated when a newer NEI was released. States release their own emissions inventories which allow partial updates to emissions. AIRPACT currently uses the 2014 NEIv2 with some local modifications or updates provided by AIRQUEST member agencies.

For biogenic emissions, the Biogenic Emissions Inventory System (BEIS3) (Vukovich & Pierce, 2002) was used in AP-3 but it was replaced with the Model of Emissions of Gases and Aerosols from Nature (MEGAN) (Guenther et al., 2006) starting with AP-4. The dataset in the BEIS3 model used a 1-km grid and was normalized by season (Chen et al., 2008). The emissions factors used in BEIS3 were based on a land use cover database for North America. Although MEGAN is designed to be used as a global emissions model for terrestrial aerosols and gases, we run MEGAN at 1-km resolution like BEIS3. According to Hogrefe et al., (2011), MEGAN can result in higher ozone concentrations because it predicts higher isoprene concentrations than BEIS3.

For wildfire emissions, AIRPACT has used the USDA Forest Service BlueSky systems. The original process depended on the USDA Forest Service BlueSky forecasts, which provided wildfire emissions and plume rise directly to AIRPACT. Several years later, the BlueSky Framework was installed and operated independently, allowing multiple options as to how emissions would be generated; the Framework offers options for each of the various steps that determine fuels, consumption, timing, and finally emissions from fires (Larkin, 2016), resulting in CO, $PM_{2.5}$, coarse PM, and heat flux projections. AIRPACT now uses the BlueSky Framework to acquire fire size and locations from SMARTFIRE, while emissions processing is streamlined through customized lookup tables and plume rise is calculated using the DEASCO3 method, which generates improved plume characterization.

BlueSky depends on SMARTFIRE (Satellite Mapping Automatic Reanalysis Tool for Fire Incident Reconciliation) to characterize fires to be modeled. SMARTFIRE gathers fire information from NOAA's Hazard Mapping System (HMS) and fire perimeters from GeoMAC (Geospatial Multi- Agency Coordination, https://www.geomac.gov) and merges them into a compatible format (Larkin, 2016). Originally, SMARTFIRE also used wildfire Incident Status Report (ICS209) fire area; however, the electronic accessibility of ICS209 reports for wildfires was transferred to an incompatible system (IRWIN). This has degraded the daily accuracy of SMARTFIRE results, especially when HMS misses fires in cloudy conditions.

As a forecast system, AIRPACT is constrained to using detected fires and thus must make assumptions. Detected fires are assumed to persist at their reported size for the two-day forecast, an assumption we refer to as 'persistence'; our inability to reflect fire suppression, fire growth, or extinguishment by weather or fuel shortage, is a limitation.

3 Results

We have evaluated the AIRPACT surface ozone levels and surface $PM_{2.5}$ concentrations at AQS sites during 2009-2018. We have also evaluated temperature, specific humidity, wind speed and direction from WRF simulations from 2009-2018, but we present those results in S-Table 1 in the supplementary materials because of the large data gap in the archived meteorology data. We used daily maximum 8-hour average (DM8A) ozone levels and daily 24 hr average $PM_{2.5}$ concentrations in all the evaluations for this paper. For ozone and $PM_{2.5}$ evaluation, we have categorized the AQS site by the location type (i.e., rural, suburban, or urban) in order to better capture any systematic forecast issues. We again note that this AIRPACT performance evaluation is limited to the common AQS sites for each species or variable, which means that if observations for a site are missing during any AIRPACT version, then we excluded that site. This reduces the number of monitoring sites, but it allows us to make a fair comparison among different AIRPACT versions: total 26 AQS sites for O_3 and total 89 sites for PM2.5 (see S-Table 2 for the details of AQS sites used in this paper).

To evaluate the AIRPACT systems forecasting accuracy progress over the time span, we used several statistical measures including mean bias (MB), mean error (ME), root mean square error (RMSE), normalized mean bias (NMB), normalized mean error (NME), fractional bias (FB), fractional error (FE), and correlation of determination (r^2). Although we present all these measures, we will mainly discuss meteorology evaluation using MB, RMSE or ME and ozone and PM2.5 evaluations using FB and FE, because of the benchmarks values available from those metrics: We obtained the benchmark values from Emery et al. (2001) for meteorology parameters and Thunis et al. (2011) for air quality parameters. Due to large gaps in the AIRPACT MCIP archived data, especially from 2009 to 2012, the AP-3 period, we provide only a brief evaluation for the meteorology forecasts and their evaluation is moved to the supplementary material.

3.1 Ozone evaluation

Table 2 shows overall forecast performance by each AIRPACT version for DM8A ozone levels at 26 AQS sites where we have O_3 measurements during the entire period (2009-2018) over the AIRPACT domain. The overall mean and 98th percentile of measured DM8A O_3 are 36 ppbv and 55 ppbv, while the forecast mean and 98th percentile are 41 ppbv and 59 ppbv, respectively. The mean bias (MB) of AIRPACT O_3 is 4.2 ppbv (fractional bias, FB, of 12%). Based on the goal benchmark value of 30% for FE and ±15% for FB used by Thunis et al.

(2011), all versions of AIRPACT show satisfactory results. Comparing among the AIRPACT versions, AP-5 performed the best (MB of 2.6 ppbv and FB of 8.1%) and AP-4 performed the worst (MB of 5.0 ppbv and FB of 14%), however AP-4 shows the highest correlation of determination (R^2) value, 0.68. From AP-3 to AP-4, most evaluation metrics values are quite similar, which indicates reducing grid spacing from 12 km to 4 km did not help to improve O_3 predictions. Updating to AP-5 shows noticeable improvements; all the bias terms are reduced by nearly a half and error terms are decreased by a few percent, even though the AP-5 version shows the lowest R^2 value, 0.54. Note that O_3 evaluation at individual AQS site is presented in S-Table 3.

Figure 1 shows ratios of forecast to measured DM8A O_3 against the corresponding measured O_3 levels at the 26 AQS sites for each AIRPACT version. Note that a ratio of 1 means perfect agreement between the forecast and measurement. All AIRPACT versions performed well, mostly within a factor of two. AIRPACT shows better agreement in higher concentration regimes (over 30 ppbv) than in lower concentration regimes (below 30 ppbv). A systematic overprediction in low concentration regimes was also reported by Chen et al. (2008), which evaluated the AIRPACT-3 during the two-month period (August and September) in 2004. This problem is also shown in other air quality models. For instance, the multi-model intercomparison study (i.e., Air Quality Model Evaluation International Initiative, AQMEII) on tropospheric ozone, presented by Im et al. (2015), found a similar systematic overprediction in surface level ozone below 30 ppbv from all participating air quality modeling systems over North America including WRF with CMAQ as is used in this study (see Figure 9b in Im et al., 2015).

To understand how AIRPACT's ability to forecast ozone has changed by seasons, we compared the observed and measured DM8A O_3 distributions by season for each AIRPACT version using a box plot (in Fig. 2). All AIRPACT versions overpredict O_3 in all season, except for the AP-5 summer season (see the details of seasonal evaluation statistics in S-Table 4). The overprediction is worse during the low O_3 season such as fall and winter (mean bias of 4.4-7.8 ppbv with fractional bias of 13-26%), compared to the high O_3 seasons such as the spring and summer (mean bias of 2.1-5.5 ppbv with fractional bias of -4.5 to 12%). The systematic overprediction of O_3 in the low concentration regime, shown in Fig. 1, should be mostly from the fall and winter seasons, as their O_3 levels are frequently below 30 ppbv. The observed highest O_3 season is not well captured for all versions: AP-4 and AP-5 show the spring as the highest while the observation shows the summer; for AP-3 peaks during the summer while the observation during the spring.

Figure 3 shows the observed and simulated diurnal ozone profiles in summer for each AIRPACT version. All AIRPACT versions capture the observed diurnal patterns remarkably well (R^2 = 0.94-0.96). The simulated max and min O_3 levels occurred at 1-2 pm and 5-6 am, respectively, which are comparable to the observation within 1-2 hours difference. Our model peak time is earlier than the observation, which also occurs in other 3-D air quality modeling systems (see Figure 8c in Im et al., 2015). The simulated O_3 max levels (45-49 ppbv) are simulated reasonably to the observation (43-47 ppbv), but our model tends to overpredict at other hours including the min levels, particularly worse during nighttime, by up to 10 ppbv. Unlike the summer O_3 diurnal profiles, no AIRPACT versions capture well the observed diurnal patterns for winter season (see Fig. 4; R^2=0.11-0.20) and all show severe overprediction during nighttime up to 17 ppbv. AIRPACT shows the max O_3 levels at 1 pm, which matches with the observation. However, the simulated min O_3 levels peak at 5pm while the observed min levels peak at 6 am. The large gaps in nighttime O_3 levels might be a common issue in air quality modeling as the multi-model inter-comparison studies by Im et al. (2015) and Solazzo et al. (2012; 2013a) also showed the same issue, which needs further investigation into what causes such high O_3 levels during the nighttime in winter.

It is important to understand what contributes to such large overprediction in low O_3 regime in air quality models, but most studies have been focused on high O_3 regime because a high O_3 level is more of concern for air quality control managements and public health. Even though a further study is needed to find those contributing factors, we suspect that this overprediction might be caused by the followings: 1) missing nighttime NO titration of O_3, especially over urban areas where the observed O3 values often go zero but the models do not predict such low O3 values; 2) incorrect background level in the models; and 3) too weak boundary layer mixing at night.

To examine the forecast skills spatially for each AIRPACT version, the FB and FE values of AIRPACT DM8A O_3 forecast performance are presented at individual AQS site in Fig. 5 and by sites grouped by location type (i.e., rural, suburban, and urban) in Fig. 6. To provide a clear picture of the overall change in FE from AP-3 to AP-5, we present the spatial distribution of FE difference in Fig. 7. The simulated DM8A O_3 levels at each AQS site span from underestimates (down to the FB of -9%) to overestimates (up to the FB of 25%) with the FE range of 10-35%. Most sites show overprediction, which changed little by the AIRPACT versions. However, the updates made to AIRPACT over the decadal period does improve the forecast performance in several sites as shown in Figs. 6f and 7. The worst performance (highest FE) tends to occur at an urban site and the best performance (lowest FE) at a rural site, but we do not find any distinct difference in overall forecast performance for those groups. Figures 6d and 6e show clearly that the model-to-observation agreement became worse from AP-3 to AP-4, despite the finer grid size applied in AP-4, and better from AP-4 to AP-5, likely because AP-5 adapted CB05 gas chemical mechanism that resulted in lower O_3 level than the SAPRC mechanism and thus alleviated one O_3 overprediction issue.

3.2 $PM_{2.5}$ evaluation

The evaluation statistical summary of AIRPACT daily $PM_{2.5}$ forecasts at 89 AQS sites for each AIRPACT version and entire 2009-2018 period are presented in Table 3. First of all, overall $PM_{2.5}$ performance is roughly twice as poor compared to the overall O_3 performance (e.g., the fractional error, FE, of O_3 and $PM_{2.5}$ are 16% and 31%, respectively). Over the major AIRPACT updates, $PM_{2.5}$ performance appears to get worse, unfortunately. For example, the FB of $PM_{2.5}$ has been increased from -4.5% to -32%, and for FE, from 26% to 38%. The coefficient of determination, R^2, is above 0.5 for all versions except for AP-4. Even though AP-5 shows the worst performance of $PM_{2.5}$ compared to previous versions, it still meets the criteria benchmark of FB, which is ± 60%. The AP-3 and AP-4 meet the goal benchmark of FB which is ± 30%. The PM2.5 evaluation at individual AQS site is presented in S-Table 5.

The ratios of forecast to measured daily $PM_{2.5}$ concentrations against the corresponding measured concentrations for each version are shown in Fig. 8. The daily $PM_{2.5}$ data points are rather equally distributed around 1 in AP-3 but started to move below 1 in the newer versions. AP-5 shows that many data points (shown as yellow colors in Fig. 8) are noticeably below 1, which reflects an underprediction issue in that version. AP-5 also has several extremely poor forecasts (i.e., ratio > 3 or ratio < 0.3), especially for the regime of $PM_{2.5}$ above 10 μg m^{-3}.

Daily PM2.5 forecast skills by each season is presented in Fig. 9. Model $PM_{2.5}$ is generally underestimated in all seasons, particularly worse during summer. Based on the benchmark values, AP-3 performed well for all seasons (FB values < ±30%). AP-4 also meets the benchmark goal for all seasons except for summer that has the FB value of -57%. In the case of AP-5, fall and winter forecasts were good but spring and summer do not meet the benchmark goals (i.e., -41% and -70%, respectively): summer does not even meet the criteria benchmark value (± 60%). The poor PM2.5 forecasts during summer seasons in AP-5 might be partly due to missing the large observed $PM_{2.5}$ spikes during the summer of 2015 and 2018, which is shown in time series plots of monthly mean PM2.5 concentrations by AQS sites (grouped by rural, suburban, and urban) in S-Fig. 3. Air quality forecasts over PNW seem to be the most challenging during summer season (wildfire season in PNW) because wildfires can result in large $PM_{2.5}$ spikes and poor air quality in a region with otherwise good air quality: the area-burn time-series plot in S-Figure 4 shows the similar pattern as PM2.5, which indicates the influence of wildfires on the spikes.

To show how the $PM_{2.5}$ forecast performed spatially for each AIRPACT major updates, we present the FB and FE values of daily $PM_{2.5}$ evaluation in a spatial distribution (Fig. 10) and in a scatter plot (Fig. 11). The spatial distribution of FE difference from AP-3 to AP-5 at individual site is shown in Fig. 12. AIRPACT $PM_{2.5}$ performance ranges from underestimates (down to the FB of -126%) to overestimates (up to the FB of 84%), with the FE range of 32-134%. As shown in Fig. 10, it tends to underpredict daily $PM_{2.5}$ across the model domain, particularly at rural areas. Unlike O_3, the daily $PM_{2.5}$ performance shows a distinct difference in overall forecast performance by site location type: rural (total 25 sites), suburban (total 34 sites), and urban (total 30 sites). The sites showing overestimates are primarily urban and suburban areas (e.g., Seattle WA and Portland OR), although some urban and suburban sites are underpredicted. Compared to the rural sites, urban and suburban sites have larger FE values. As shown in Figs. 11 and 12, the AIRPACT's $PM_{2.5}$ FE has increased with each major update; the differences of FE from AP-3 to AP-5 (in Fig. 12) are positive over most sites. This worsening of FE in AP-5 could be attributed to a) the summer of 2015 and 2018 where our model missed large PM2.5 concentrations from wildfires and b) use of the monthly mean chemical boundary condition during February 2, 2018 to October 31, 2018 because the MOZART4 from NCAR was discontinued; otherwise, it is likely that AP-5 may have a similar performance as previous versions, if not better.

4 Conclusion

Since May 2001, the Laboratory for Atmospheric Research (LAR) group at Washington State University has been operating the AIRPACT air quality forecast system that predicts immediate future air quality over the PNW region. Currently, we are running the AIRPACT version 5 (AP-5) which forecasts the next 48 hours of high-resolution air quality over the PNW region. Our AIRPACT system comprises three main models: WRF meteorology model, SMOKE emission processing tool, and CMAQ chemical transport model. The CMAQ simulations in AIRPACT use a comprehensive set of emissions that is based on up-to-date emission inventories (i.e., EPA's NEI2014v2 and new state emission inventories) and emission models such as MOVES mobile emission model, MEGAN biogenic emission model, and BlueSky fire emission model.

In this paper, we have evaluated the last 10 years of archived AIRPACT forecast data, from 2009 to 2018, against the EPA's AQS monitoring sites. Our evaluation is limited to the forecast products at the EPA's AQS sites. Over this time period, the AIRPACT system went through two major updates that resulted in system version change: from AP-3 (2007 to 2012) to AP-4 (2013 to 2015) and to AP-5 (2016 to present). The major updates made to the AIRPACT system include: a) incorporating newer model versions for CMAQ, WRF, and SMOKE; b) switching to a different chemical mechanism (e.g., from SAPRC99 to CB05) or to a different sub-model (from MOBILE6 to MOVES; from BEIS to MEGAN); c) using finer horizontal and vertical grids; and d) adapting newer input dataset such as emission inventories and chemical boundary conditions (see the details in Table 1).

AIRPACT O_3 forecasting has improved over time. Between AP-3 and AP-4 there are minimal forecast skill differences; however, the update to AP-5 showed notable improvements. AP-5 is improved from AP-3 and AP-4 according to all statistical metrics used, excluding R^2. In AP-5, the MB and FB are nearly twice as good compared to either preceding version. The switch to CB05 gas chemical mechanism from SAPRC99 lowered the forecasted O_3 levels and thus lessened AIRPACT's tendency to overpredict O_3, which likely explains the better performance of AP-5. For all versions of AIRPACT, the FB and FE have met the goal benchmark values (i.e., FB of ±15 % and FE of ±30%) for O_3. We find that O_3 levels above 30 ppbv were forecasted with higher accuracy than levels below 30 ppbv and O_3 forecast performance is generally better in the summer than in the winter, including their diurnal cycles. All versions of AIRPACT struggle at forecasting wintertime O_3, with constant overprediction, especially during the night.

Unlike the O_3 forecast performance, as AIRPACT has progressed through versions, the $PM_{2.5}$ forecast performance has worsened from slight overprediction (FB of 4.5%) in AP-3 to large underprediction (FB of -32%) in AP-5. The poor performance of $PM_{2.5}$ in AP-5 was likely due to the large underpredictions during spring and summer that are contributed by missing wildfires emissions and using monthly mean chemical boundary condition. However, all versions of AIRPACT meet the criteria benchmark for FB of ± 60%.

It is important to understand that our comparisons between different AIRPACT versions are not based on the same period and thus the changes in forecast skills over time are also influenced by the changes in extreme air quality events such as stratospheric ozone intrusion and wildfires. For example, the significant underprediction of $PM_{2.5}$ in AP-5 is attributed to the summers of 2015 and 2018; where the AP-5 forecast severely underpredicted large $PM_{2.5}$ concentrations due to wildfires. The PM2.5 underprediction in summer 2018 were largely due to missing smoke from Canadian fires in the chemical boundary conditions: we were using archived monthly mean chemical boundary conditions as MOZART was no longer available and it was before our transition to WACCM. This suggests that a more reliable forecast system to handle extreme air quality events may improve overall forecast accuracy.

This multi-year evaluation provides a unique opportunity to examine how a regional air quality system has evolved over the last 10 years, particularly how the substantial science advances and technical updates applied to the system have affected air quality forecast ability. Even though our long-term evaluation reveals that some major updates such as reducing grid size did not improve the forecast skills, the updates made to the system have been based on the latest science, to the best of our knowledge, and thus AIRPACT has evolved into a more advanced air quality forecast system over time. Compared to the substantial efforts went into the AIRPACT updates, our forecast accuracy has improved little, which reflects the challenges in improving forecast skills in the current AIRPACT system that is based on 3-D air quality modeling alone. This finding suggests the need to consider new approaches including data-assimilation, ensemble forecasting, and statistical post-processing that accounts for systematic model errors and sub-grid processes.

5 References

Beardsley, M., Warila, J., Dolce, G., & Koupal, J. (2009). *Air Pollution Emissions from Highway Vehicles: What MOVES Tells Us*.

Chen, J., Vaughan, J., Avise, J., O'Neill, S., & Lamb, B. (2008). Enhancement and evaluation of the AIRPACT ozone and PM $_{2.5}$ forecast system for the Pacific Northwest. *Journal of Geophysical Research*, *113*(D14). https://doi.org/10.1029/2007JD009554

Emery, C., Tai, E., & Yarwood, G. (2001). *Enhanced meteorological modeling and performance evaluation for two Texas ozone episodes*. Prepared for the Texas natural resource conservation commission, by ENVIRON International Corporation.

Fann, N., Lamson, A. D., Anenberg, S. C., Wesson, K., Risley, D., & Hubbell, B. J. (2012). Estimating the National Public Health Burden Associated with Exposure to Ambient PM2.5 and Ozone. *Risk Analysis*, *32*(1), 81–95. https://doi.org/10.1111/j.1539-6924.2011.01630.x

Guenther, A., Karl, T., Harley, P., Wiedinmyer, C., Palmer, P. I., & Geron, C. (2006). Estimates of global terrestrial isoprene emissions using MEGAN (Model of Emissions of Gases and Aerosols from Nature). *Atmospheric Chemistry and Physics*, *6*(11), 3181–3210.

Herron-Thorpe, F. L., Lamb, B. K., Mount, G. H., & Vaughan, J. K. (2010). Evaluation of a regional air quality forecast model for tropospheric NO2 columns using the OMI/Aura satellite tropospheric NO2 product. *Atmos. Chem. Phys.*, 16.

Herron-Thorpe, F. L., Mount, G. H., Emmons, L. K., Lamb, B. K., Jaffe, D. A., Wigder, N. L., Chung, S. H., Zhang, R., Woelfle, M. D., & Vaughan, J. K. (2014). Air quality simulations of wildfires in the Pacific Northwest evaluated with surface and satellite observations during the summers of 2007 and 2008. *Atmospheric Chemistry and Physics*, *14*(22), 12533–12551. https://doi.org/10.5194/acp-14-12533-2014

Hogrefe, C., Isukapalli, S. S., Tang, X., Georgopoulos, P. G., He, S., Zalewsky, E. E., Hao, W., Ku, J.-Y., Key, T., & Sistla, G. (2011). Impact of biogenic emission uncertainties on the simulated response of ozone and fine particulate matter to anthropogenic emission reductions. *Journal of the Air & Waste Management Association (1995)*, *61*(1), 92–108.

Im, U., Bianconi, R., Solazzo, E., Kioutsioukis, I., Badia, A., Balzarini, A., Baró, R., Bellasio, R., Brunner, D., Chemel, C., Curci, G., Flemming, J., Forkel, R., Giordano, L., Jiménez-Guerrero, P., Hirtl, M., Hodzic, A., Honzak, L., Jorba, O., … Galmarini, S. (2015). Evaluation of operational on-line-coupled regional air quality models over Europe and North America in the context of AQMEII phase 2. Part I: Ozone. *Atmospheric Environment*, *115*, 404–420. https://doi.org/10.1016/j.atmosenv.2014.09.042

Jaffe, D., Anderson, T., Covert, D., Kotchenruther, R., Trost, B., Danielson, J., Simpson, W., Berntsen, T., Karlsdottir, S., Blake, D., Harris, J., Carmichael, G., & Uno, I. (1999). Transport of Asian air pollution to North America. *Geophysical Research Letters*, *26*(6), 711–714. https://doi.org/10.1029/1999GL900100

Koupal, J., Cumberworth, M., Michaels, H., Beardsley, M., & Brzezinski, D. (2003). *Design and Implementation of MOVES: EPA's New Generation Mobile Source Emission Model*. 15.

Larkin, S. (2016, November 9). *Wildland Fire Assessment Tools: SmartFire and BlueSky*. http://www.westar.org/Docs/EEworkshop/Larkin.pdf

Luecken, D. J., Phillips, S., Sarwar, G., & Jang, C. (2008). Effects of using the CB05 vs. SAPRC99 vs. CB4 chemical mechanism on model predictions: Ozone and gas-phase photochemical precursor concentrations. *Atmospheric Environment*, *42*(23), 5805–5820. https://doi.org/10.1016/j.atmosenv.2007.08.056

Mahmud, A. (2005). *EVALUATION OF THE AIRPACT2 AIR QUALITY FORECAST SYSTEM FOR THE PACIFIC NORTHWEST* [Washington State University]. https://research.libraries.wsu.edu/xmlui/bitstream/handle/2376/402/a_mahmud_091605.pdf?sequence=1

Mass, C. F., Albright, M., Ovens, D., Steed, R., Maciver, M., Grimit, E., Eckel, T., Lamb, B., Vaughan, J., Westrick, K., Storck, P., Colman, B., Hill, C., Maykut, N., Gilroy, M., Ferguson, S. A., Yetter, J., Sierchio, J. M., Bowman, C., … Brown, W. (2003). Regional Environmental Prediction Over the Pacific Northwest. *Bulletin of the American Meteorological Society*, *84*(10), 1353–1366. https://doi.org/10.1175/BAMS-84-10-1353

Neidell, M. (2004). Air pollution, health, and socio-economic status: the effect of outdoor air quality on childhood asthma. *Journal of Health Economics*, *23*(6), 1209–1236. https://doi.org/10.1016/j.jhealeco.2004.05.002

Thunis, P., Georgieva, E., & Galmarini, S. (2011). *A procedure for air quality models benchmarking, Version 2*.

US EPA. (2015a, May 29). *The Clean Air Act - Highlights of the 1990 Amendments* [Overviews and Factsheets]. US EPA. https://www.epa.gov/clean-air-act-overview/clean-air-act-highlights-1990-amendments

US EPA, O. (2015b, June 2). *National Emissions Inventory (NEI)* [Policies and Guidance]. US EPA. https://www.epa.gov/air-emissions-inventories/national-emissions-inventory-nei

US EPA, O. (2016, June 1). *Description and History of the MOBILE Highway Vehicle Emission Factor Model* [Overviews and Factsheets]. US EPA. https://www.epa.gov/moves/description-and-history-mobile-highway-vehicle-emission-factor-model

Vaughan, J., Lamb, B., Frei, C., Wilson, R., Bowman, C., Figueroa-Kaminsky, C., Otterson, S., Boyer, M., Mass, C., Albright, M., Koenig, J., Collingwood, A., Gilroy, M., & Maykut, N. (2004). A Numerical Daily Air Quality Forecast System for The Pacific Northwest. *Bulletin of the American Meteorological Society*, *85*(4), 549–562. https://doi.org/10.1175/BAMS-85-4-549

Vukovich, J. M., & Pierce, T. (2002). Implementation of BEIS3 within the SMOKE modeling framework. *Proceedings of the 11th International Emissions Inventory Conference, Atlanta, Georgia*, 15–18.

WHO. (2016). *WHO | Ambient air pollution: A global assessment of exposure and burden of disease*. WHO. http://www.who.int/phe/publications/air-pollution-global-assessment/en/

6 Acknowledgements

This work has been supported by the NW-AIRQUEST consortium of air quality agencies in the Pacific Northwest.

Decadal Evaluation of the AIRPACT Regional Air Quality Forecast System in the Pacific Northwest from 2009-2018

Jordan A. Munson[1#], Joe Vaughan[1], Brian Lamb[1], and Yunha Lee[1*]

[1]Laboratory for Atmospheric Research Civil and Environmental Engineering, Washington State University, Pullman, 99163, United States

[#]now at Wisconsin Department of Natural Resources, Madison, WI 53707-7921
[*]now at Center for Advanced Systems Understanding, Helmholtz-Zentrum Dresden–Rossendorf, Dresden, Germany

Correspondence to: Yunha Lee (y.lee@hzdr.de)

Figures and Tables are presented in this document.

Table 1. Description of the AIRPACT systems used from 2009 to 2018

	Category	**AIRPACT-3 (AP-3)**	**AIRPACT-4 (AP-4)**	**AIRPACT-5 (AP-5)**
	Duration	2007- Dec 2012	Jan 2013 – Dec 2015	Jan 2016 - Current
	Horizontal grid size	12-km	4-km	4-km
	Number of vertical layers	21	21	37
	Meteorology model	MM5 3.7.3 (before April 2008), WRF v3.1.1	WRF v3.4.1, v3.5	WRF v3.6.1, v3.7.1
	MCIP	v3.3	v3.6	v3.6
	SMOKE emission tool	v2.1	v2.7, v3.5	v3.5.1
CMAQ	CMAQ version	v4.6	v4.7.1	v5.0.2
CMAQ	Mass Adjustment (CMAQ)	denrate	yamo	yamo
CMAQ	Gas-Phase Mechanism	SAPRC99	SAPRC99	CB05
CMAQ	Non-mobile Anthropogenic Emissions	2005 from Ecology, IDEQ, ODEQ	2007-2008 from Ecology, IDEQ, ODEQ	NEI 2014v2
CMAQ	Mobile Emissions	MOBILE6	MOBILE6, MOVES	MOVES 2010b
CMAQ	Fire Emissions	BlueSky	SMARTFirev1/BlueSky SMARTFire v2, BlueSky 3.5.1 (2014 and later)	SMARTFire v2, BlueSky 3.5.1
CMAQ	Biogenic Emissions	BEIS-3	MEGAN v2.0.4	MEGAN v2.1
CMAQ	Boundary Conditions	MOPITT CO Assimilated MOZART-4 Forecast from LOUISA Emmons of NCAR	MOPITT CO Assimilated MOZART-4 Forecast from LOUISA Emmons of NCAR	MOZART4 ceased ~Jan 2018, since then Monthly averaged from 2014

Table 2. Statistical results of daily maximum 8-hour average (DM8A) ozone performance at the EPA AQS sites in the AIRPACT domain that from 2009 to 2018. Values shown are for the entire duration of the corresponding AIRPACT version.

AIRPACT Version	Forecast Mean [ppb]	Forecast 98th [ppb]	Observation Mean [ppb]	Observation 98th [ppb]	MB [ppb]	ME [ppb]	FB [%]	FE [%]	NMB [%]	NME [%]	RMSE [ppb]	R2 [-]
AP-3	40	57	36	52	4.7	5.7	14	17	13	16	7.1	0.67
AP-4	42	63	37	55	5.0	6.0	14	17	14	16	7.7	0.68
AP-5	40	56	37	56	2.6	4.9	8.1	14	7.0	13	6.8	0.54
Overall	41	59	36	55	4.2	5.6	12	16	11	15	7.2	0.62

Table 3. Same as Table 2 but for daily $PM_{2.5}$ concentrations

AIRPACT Version	Forecast		Observation		MB [μg m^{-3}]	ME [μg m^{-3}]	FB [%]	FE [%]	NMB [%]	NME [%]	RMSE [μg m^{-3}]	R2 [-]
	Mean [μg m^{-3}]	98th [μg m^{-3}]	Mean [μg m^{-3}]	98th [μg m^{-3}]								
AP-3	6.8	19.1	7.0	16.8	-0.2	1.9	-4.5	26	-2.5	27	2.6	0.59
AP-4	6.5	18.0	7.7	20.6	-1.3	2.1	-18	28	-16	27	3.7	0.48
AP-5	6.0	18.4	7.8	30.4	-1.8	2.7	-32	38	-23	34	5.8	0.55
Overall	6.5	18.3	7.5	20.6	-1.0	2.2	-17	31	-13	29	4.2	0.53

Table 4. Summary of forecast verification metrics for ozone and $PM_{2.5}$ air quality index (AQI). FAR stands for False Alarm Ratio and POD for Probability of Detection. AQI rows are based on the full spectrum of AQI values, whereas the unit value rows are based on a single value ceiling.

Species		Metric	AP-3	AP-4	AP-5
O_3	AQI	FAR	0.035	0.10	0.02
		POD	1.0	0.99	0.98
	> 27 ppb	FAR	0.91	0.80	0.83
		POD	0.96	0.89	0.75
PM2.5	AQI	FAR	0.043	0.034	0.024
		POD	0.96	0.93	0.93
	> 6 µg m^{-3}	FAR	0.21	0.076	0.054
		POD	0.76	0.72	0.80

The FAR has an ideal value of zero, and the POD has an ideal value of one. The FAR describes how often the forecast predicted a higher AQI than observations. The POD describes how often the forecast predicted a lower AQI than observation.

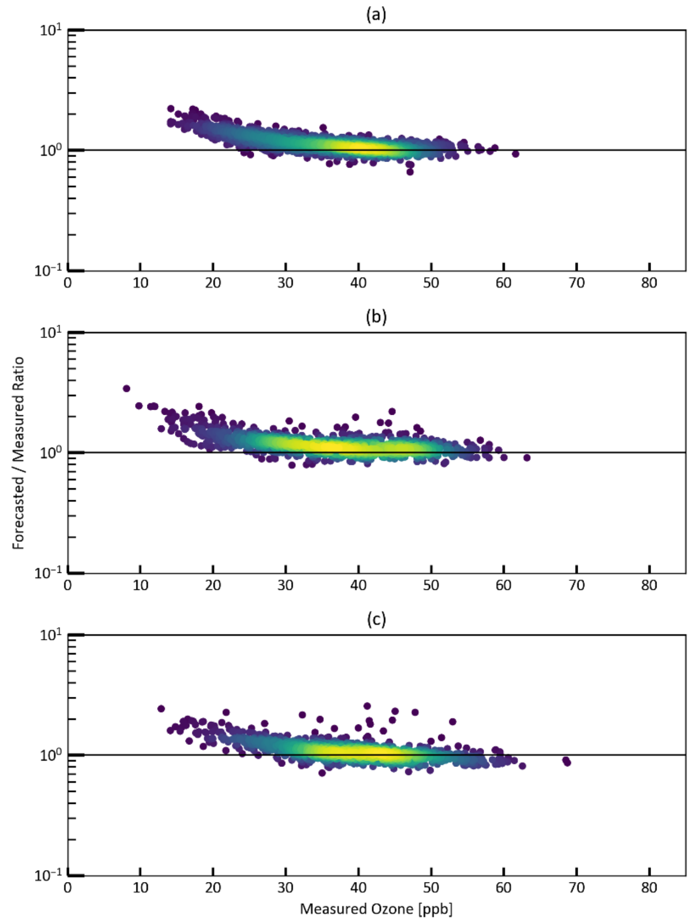

Figure1. Ratio of forecasted to measured DM8A ozone against measured values for AP-3 (a), AP-4 (b), and AP-5 (c).

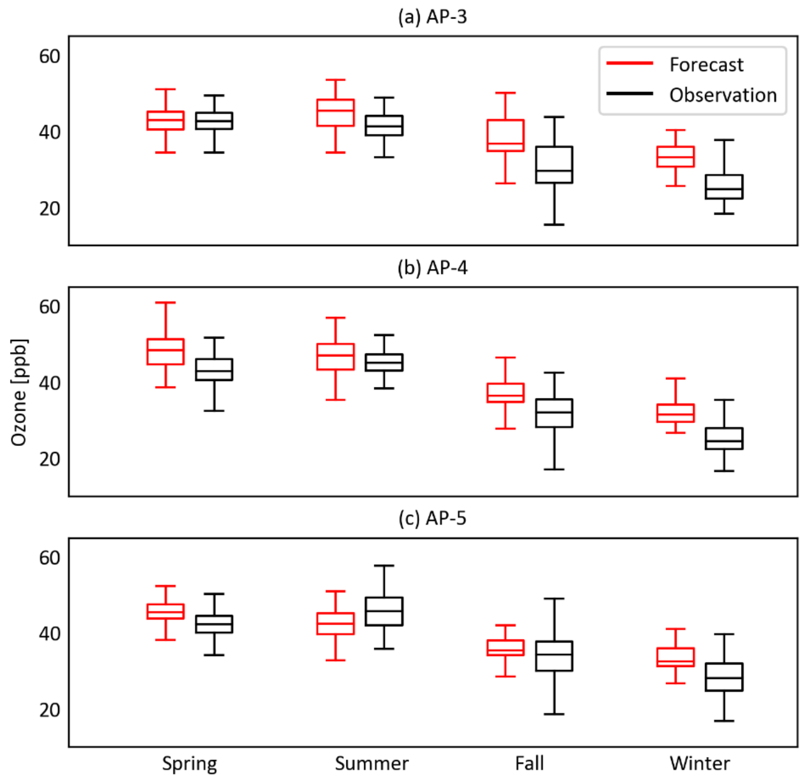

Figure 2. Boxplots of the AIRPACT MD8A ozone during AP-3 (a), AP-4 (b), and AP-5 (c). Within the plots the top whisker, top line, middle line, bottom line, and bottom whisker represent the 4th quartile, 3rd quartile, median, 2nd quartile, and 1st quartile respectively.

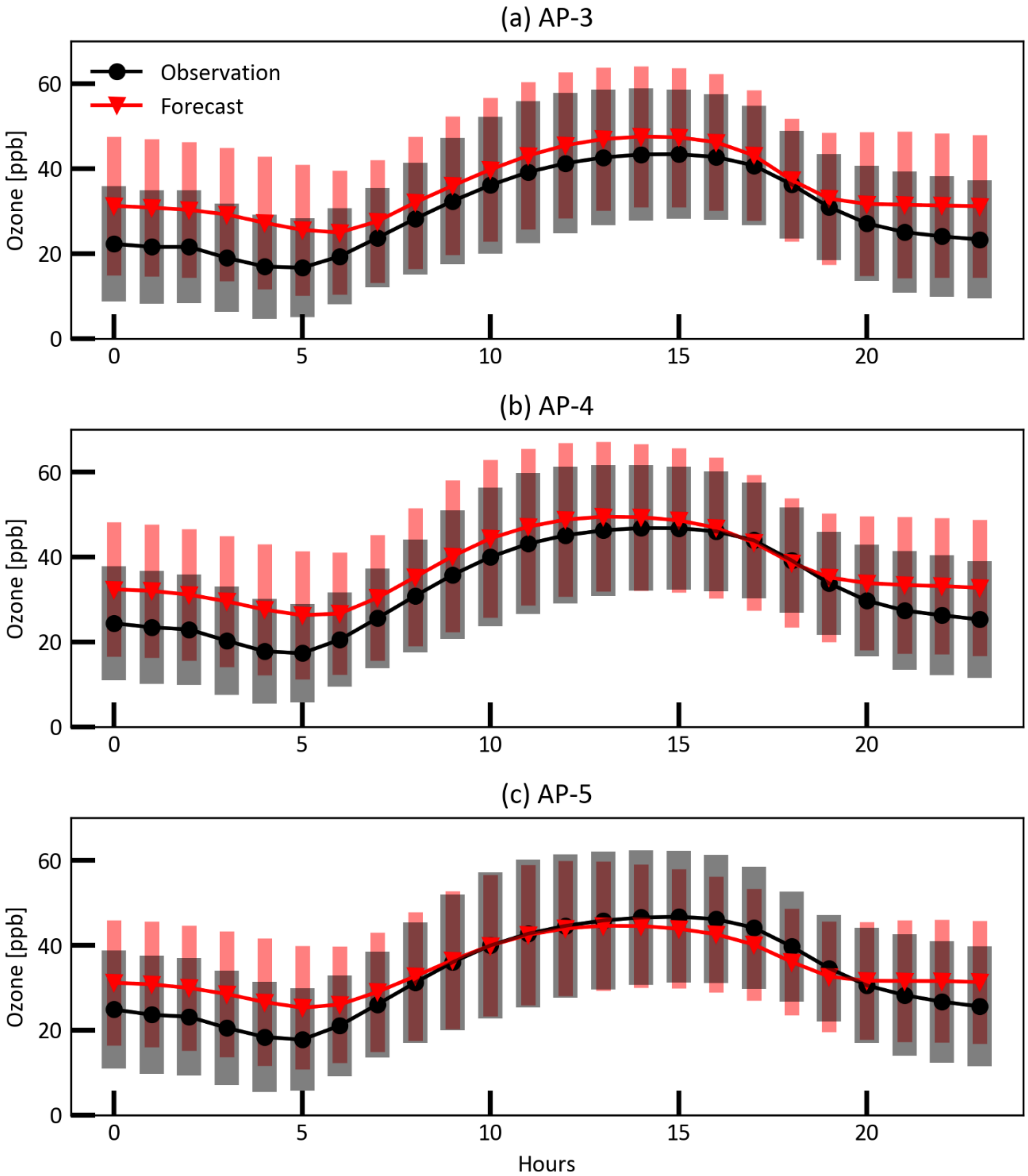

Figure 3. Observed and simulated summertime diurnal ozone concentrations at 26 common sites for AP-3 (a), AP-4 (b), and AP-5 (c). The lines represent average concentration while the shaded boxes are standard deviation.

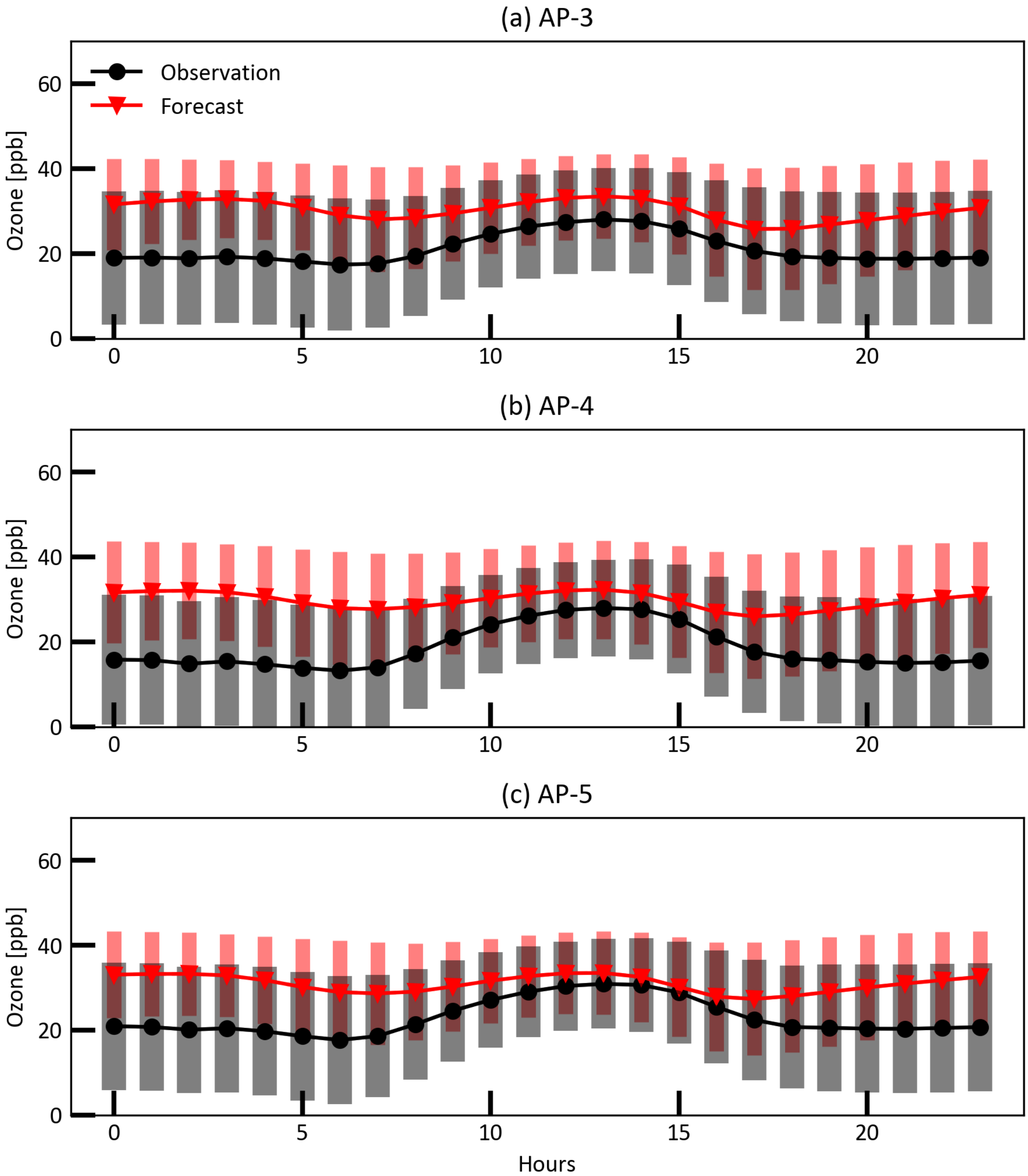

Figure 4. Observed and simulated wintertime diurnal ozone concentrations at 26 common sites for AP-3 (a), AP-4 (b), and AP-5 (c). The lines represent average concentration while the shaded boxes are standard deviation.

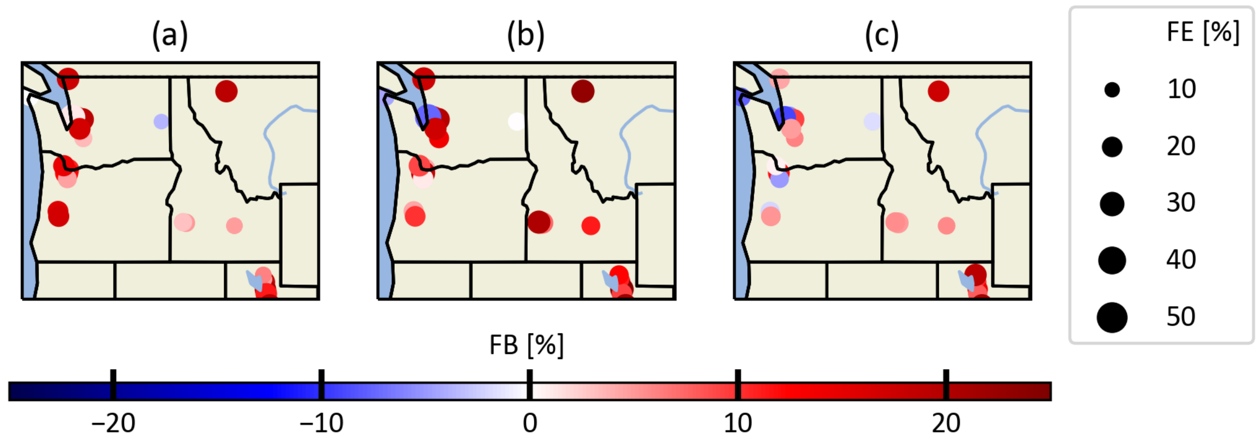

Figure 5. Spatial distribution of DM8A ozone fractional bias (FB) and fractional error (FE) of AP-3 (a), AP-4 (b), and AP-5 (c). At each monitor site, FB is represented by color bar and FE is represented by circle size.

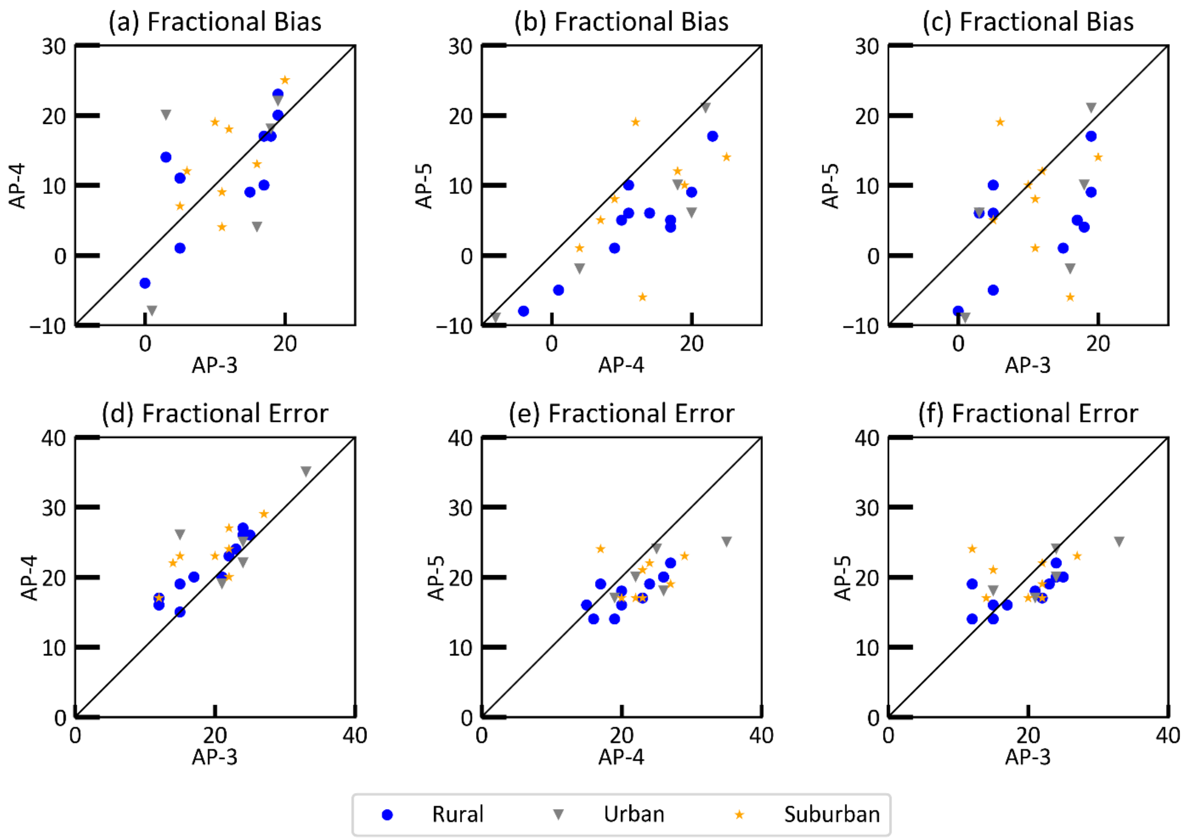

Figure 6. DM8A ozone scatter plots of fractional bias (FB) and fractional error (FE) between two AIRPACT versions at monitor sites. Blue, orange, and grey circles represent rural, suburban and urban sites, in respectively.

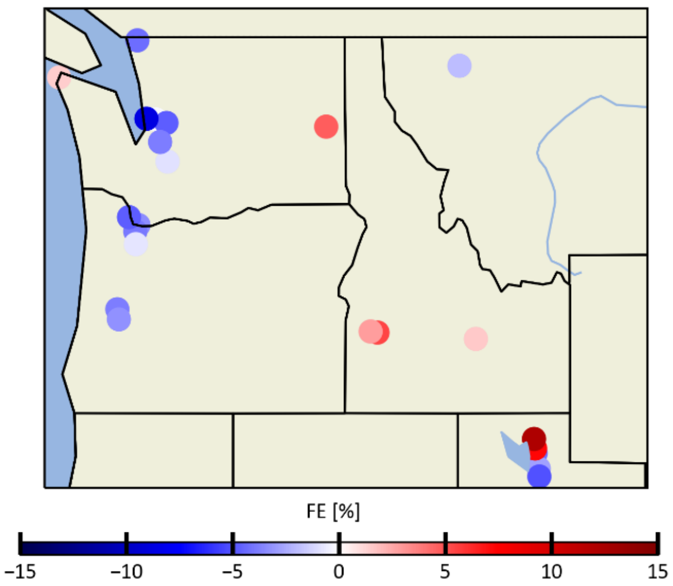

Figure 7. Spatial distribution of DM8A Ozone fractional bias (FE) difference between AP-5 and AP-3 At each monitor site, FE is represented by color bar.

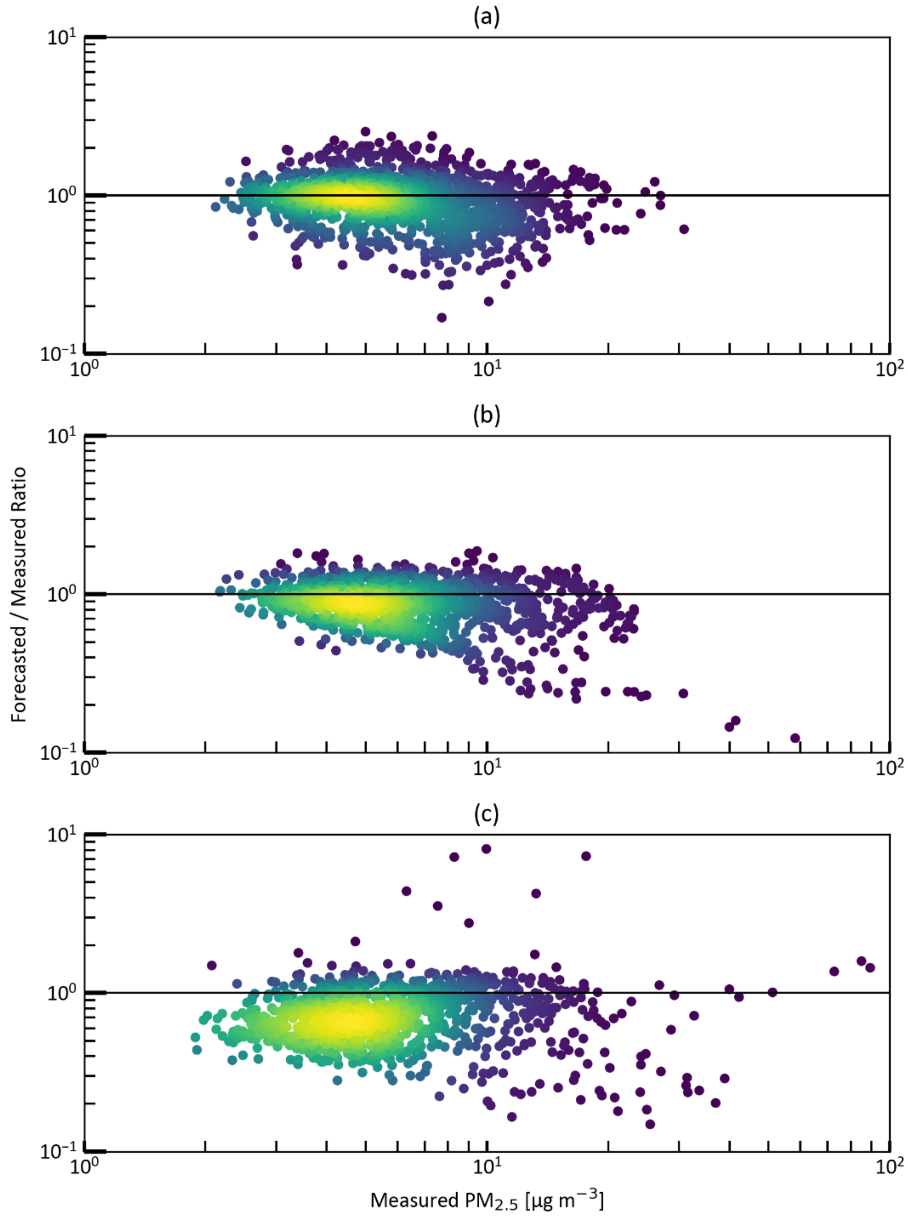

Figure 8. Ratio of forecasted to measured daily $PM_{2.5}$ against measured values for AP-3 (a), AP-4 (b), and AP-5 (c).

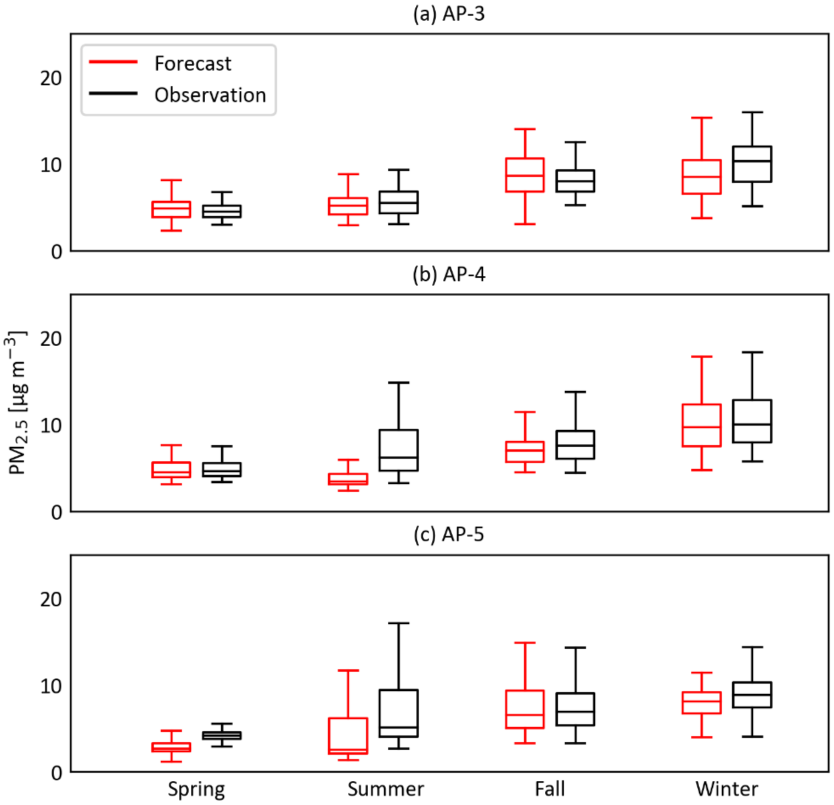

Figure 9. Boxplots of the AIRPACT daily $PM_{2.5}$ average during AP-3 (a), AP-4 (b), and AP-5 (c). Within the plots the top whisker, top line, middle line, bottom line, and bottom whisker represent the 4th quartile, 3rd quartile, median, 2nd quartile, and 1st quartile respectively.

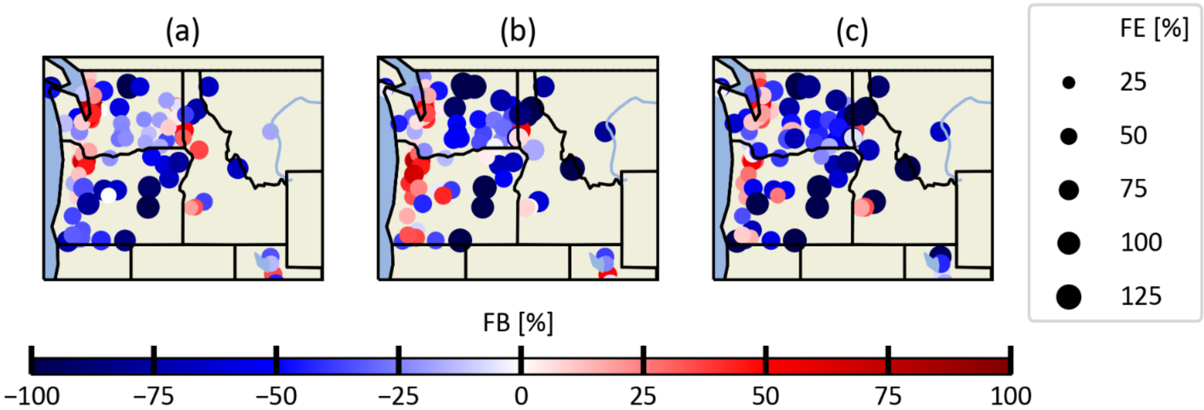

Figure 10. Spatial distribution of daily PM2.5 fractional bias (FB) and fractional error (FE) of AP-3 (a), AP-4 (b), and AP-5 (c). At each monitor site, FB is represented by color bar and FE is represented by circle size.

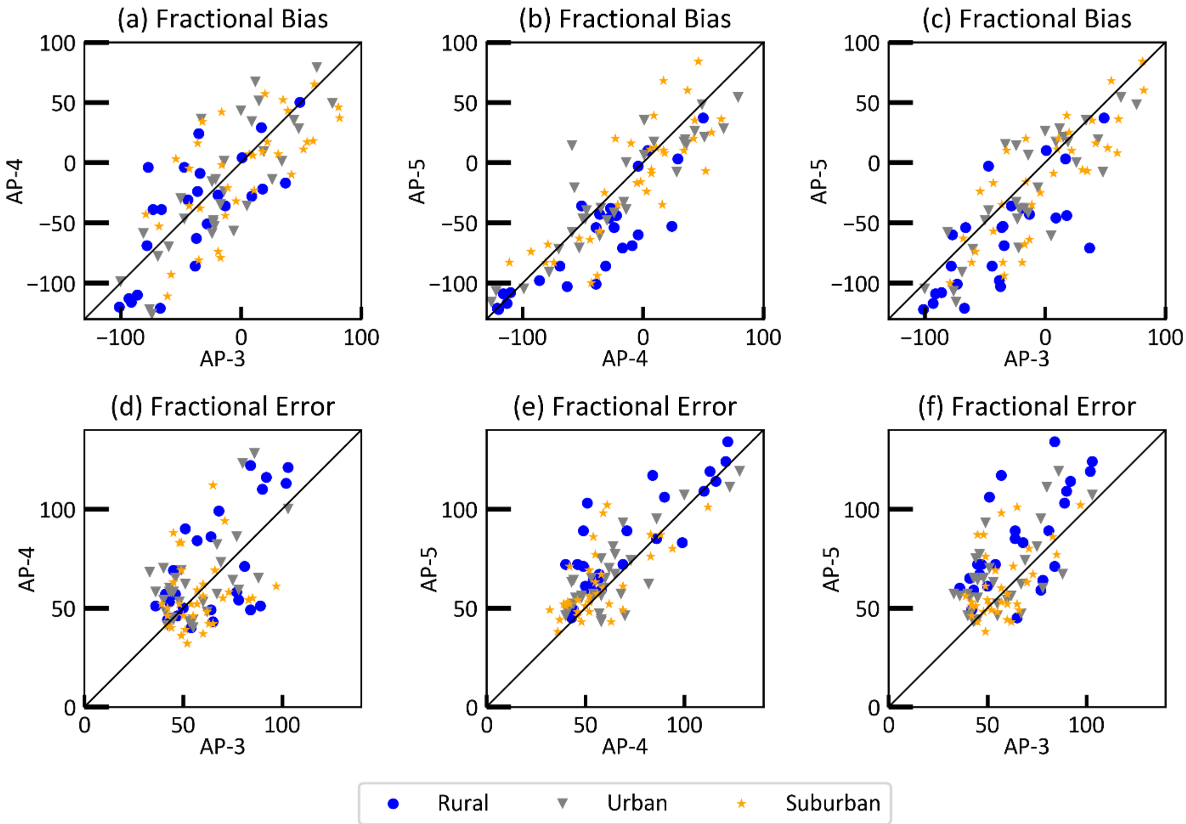

Figure 11. $PM_{2.5}$ scatter plots of fractional bias (FB) and fractional error (FE) between two AIRPACT versions at monitor sites. Blue, orange, and grey circles represent rural, suburban and urban sites, in respectively.

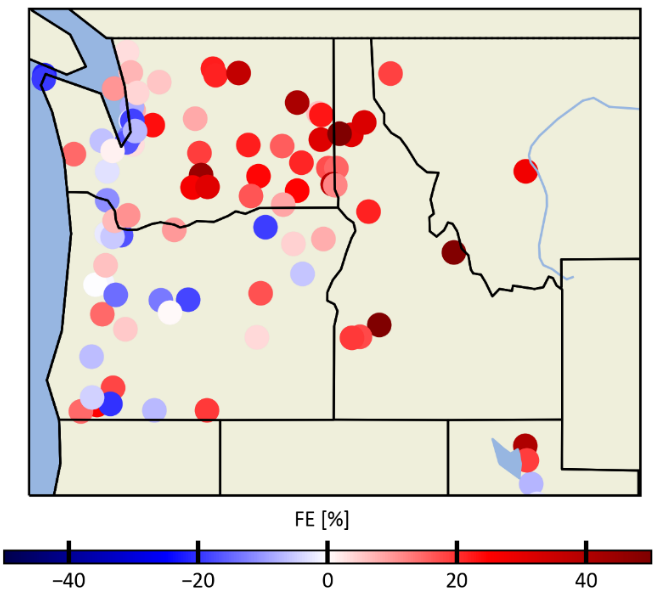

Figure 12. Spatial distribution of daily $PM_{2.5}$ fractional bias (FE) difference between AP-5 and AP-3 at each monitor site, FE is represented by color bar.

This is a non peer-reviewed preprint submitted to EarthArxiv.

Supplementary materials

Decadal Evaluation of the AIRPACT Regional Air Quality Forecast System in the Pacific Northwest from 2009-2018

Jordan A. Munson[1#], Joe Vaughan[1], Brian Lamb[1], and Yunha Lee[1*]

[1]Laboratory for Atmospheric Research Civil and Environmental Engineering, Washington State University, Pullman, 99163, United States

[#]now at Wisconsin Department of Natural Resources, Madison, WI 53707-7921
[*]now at Center for Advanced Systems Understanding, Helmholtz-Zentrum Dresden–Rossendorf, Dresden, Germany

Correspondence to: Yunha Lee (y.lee@hzdr.de)

AIRPACT forecasting system has been using the Weather Research and Forecasting (WRF) model to simulate meteorology fields which are inputs for CMAQ. WRF is operated by University of Washington and their outputs are transferred to Washington State University to perform AIRPACT forecasts. The WRF model used in AIRPACT has been updating multiple times during 2009-2018, from WRF v3.1.1 to WRF v3.7.1 Compared to WRF v3.1.1 used in AP-3, WRF v3.4.1 used in AP-4 had a newer YSU PBL scheme, which improved nighttime eddy diffusivity and thus surface temperature predictions (Hu, Klein, & Xue, 2013). WRF v3.4.1 was replaced with WRF v3.5 during AP-4, but these WRF updates made little change in AIRPACT forecast: it is based on the previous work done in our group, but not published. With the update to WRF v3.6.1 used for the early period of AP-5 (from WRF v3.5 in AP-4), the land surface model component of WRF was changed from the Noah Land Surface Model (NOAH) to the NOAH Multi Physics (NOAH MP) model. NOAH MP handles vegetation differently, with separate top and bottom canopies, and has a more in depth hydrologic component, allowing a more accurate representation of the surface when covered in snow (Niu et al., 2011).

Due to the long-term storage issues, we lost some archived meteorology forecasts, which hinder the portion of the meteorology analysis. We still evaluated WRF performances against the observation at EPA AQS sites, which are compared to two sets of benchmark values: simple case benchmark from Emery et al. (2001) and complex case benchmark from McNally et al. (2009) (shown in S-Table 1). First of all, specific humidity and wind direction are well within the simple case benchmark values for all three AIRPACT versions. Wind speed performance are slightly worse than the simple MB benchmark values (i.e., –0.5 m s-

^{1}) but is well within the RMSE benchmark (i.e., ±2 m s^{-1}). Temperature is shown to be the least satisfactory, as it even falls out of the complex case MB benchmark value (i.e., ±2.0 K) before the AP-5 period.

Updates made into the WRF model does not necessarily improve meteorology forecasts in all aspect. Based on the ME/RMSE values, wind speed and wind direction are improved approximately by 10-30% from AP-3 to AP-4 and by 0-15% from AP-4 to AP-5. Temperature and humidity are worsened approximately by 40-130% from AP-3 to AP-4, although it is improved by 30-60% from AP-4 to AP-5. The poor performance in temperature and humidity in AP-4, compared to AP-3, is rather unexpected as the grid resolution was changed from 12 km x 12 km to 4 km x 4 km along with other updates.

S-Table 1. Statistical results of WRF performance at EPA AQS sites in the AIRPACT domain from 2009 to 2018 that compared to the benchmark values obtained from Emery et al. (2001) and McNally et al. (2009). For the model values falling out of the benchmark, it is marked as red color.

Parameter		Benchmark (simple)	Benchmark (complex)	AP-3	AP-4	AP-5
Temperature (Temp) [K]	MB	≤ ±0.5	≤ ±2.0	-2.1	-3.1	-1.2
	ME	≤ ±2	≤ ±3.5	2.3	3.3	1.2
Wind speed (WS) [m s^{-1}]	MB	≤ ±0.5	≤ ±1.5	-0.64	-0.52	-0.58
	RMSE	≤ ±2	≤ ±2.5	0.94	0.65	0.65
Wind Direction (WD) [deg]	MB	≤ ±10	N/A	-1.7	-1.1	2.4
	ME	≤ ±30	≤ ±55	9.2	8.4	7.1
Humidity [g kg^{-1}]	MB	≤ ±1	N/A	0.01	-0.13	-0.04
	ME	≤ ±2	N/A	0.15	0.35	0.23

S-Table 2. List of common AQS sites used.

Species	AQSID	Latitude	Longitude	Site Type	Site Name
O_3	530090013	48.29786	-124.625	RURAL	CHEEKA PEAK
O_3	300298001	48.5103	-113.997	RURAL	GLACIER NATIONAL PARK
O_3	490571003	41.30361	-111.988	RURAL	Harrisville
O_3	160010010	43.6007	-116.348	URBAN AND CENTER CITY	St. Luke's Meridian
O_3	410090004	45.76853	-122.772	RURAL	SAUVIE ISLAND-SIS

O_3	490490002	40.25361	-111.663	URBAN AND CENTER CITY	North Provo
O_3	530330017	47.49022	-121.773	RURAL	NORTH BEND - NORTH BEND WAY
O_3	410050004	45.25928	-122.588	RURAL	CARUS TRAILER/SPANGLER RD
O_3	490495010	40.13634	-111.661	SUBURBAN	Spanish Fork
O_3	530630001	47.41645	-117.53	N/A	CHENEY - TURNBULL
O_3	530530012	46.7841	-121.74	RURAL	MT RAINIER - JACKSON VISITIORS CENTER
O_3	410390060	44.02631	-123.084	URBAN AND CENTER CITY	Eugene - AMAZON PARK (EAP)
O_3	530330080	47.56824	-122.309	URBAN AND CENTER CITY	SEATTLE - BEACON HILL
O_3	410510080	45.49664	-122.603	SUBURBAN	Portland - SE Lafayette
O_3	530330023	47.1411	-121.938	RURAL	ENUMCLAW - MUD MTN (Army Corp of Engineers site)
O_3	490110004	40.90297	-111.884	SUBURBAN	Bountiful Viewmont
O_3	530110011	45.61667	-122.517	SUBURBAN	VANCOUVER - BLAIRMONT DR
O_3	490030003	41.49271	-112.019	SUBURBAN	Brigham City
O_3	160010017	43.5776	-116.178	SUBURBAN	SAMPLER LOCATED ON SCHOOL ROOF-TOP IN SUBURBAN MOSTLY RESDNT'L AREA
O_3	410391007	43.8345	-123.035	RURAL	Eugene - Saginaw
O_3	490353006	40.73639	-111.872	SUBURBAN	Hawthorne
O_3	160230101	43.46056	-113.562	RURAL	Craters of the Moon National Monument, Visitor Center
O_3	530730005	48.95074	-122.554	RURAL	CUSTER - LOOMIS
O_3	490570002	41.20632	-111.976	URBAN AND CENTER CITY	Ogden
O_3	530330010	47.5525	-122.065	SUBURBAN	ISSAQUAH - LAKE SAMMAMISH (Wiithin Lake Sammamish State Park)
$PM_{2.5}$	530150015	46.13944	-122.962	SUBURBAN	LONGVIEW - 30TH AVE
$PM_{2.5}$	410610119	45.339	-118.095	URBAN AND CENTER CITY	LA GRANDE ASH STREET
$PM_{2.5}$	530610005	47.8064	-122.317	SUBURBAN	LYNNWOOD - 212TH
$PM_{2.5}$	160090010	47.31658	-116.571	URBAN AND CENTER CITY	USFS AT CENTER AND 9TH ST, ST. MARIES, BENEWAH COUNTY.

$PM_{2.5}$	410170120	44.06392	-121.313	URBAN AND CENTER CITY	OPEN FIELD/RESIDENTIAL AREA BY DESCHUTES RIVER. CITY PUMP STATION.
$PM_{2.5}$	530470009	48.36451	-120.121	RURAL	TWISP - GLOVER ST
$PM_{2.5}$	530531018	47.14	-122.3	SUBURBAN	PUYALLUP - 128TH ST
$PM_{2.5}$	530330017	47.49022	-121.773	RURAL	NORTH BEND - NORTH BEND WAY
$PM_{2.5}$	410050004	45.25928	-122.588	RURAL	CARUS TRAILER/SPANGLER RD
$PM_{2.5}$	410470041	44.94311	-123.006	URBAN AND CENTER CITY	Salem - State Hospital
$PM_{2.5}$	410390060	44.02631	-123.084	URBAN AND CENTER CITY	Eugene - AMAZON PARK (EAP)
$PM_{2.5}$	530330080	47.56824	-122.309	URBAN AND CENTER CITY	SEATTLE - BEACON HILL
$PM_{2.5}$	410510080	45.49664	-122.603	SUBURBAN	Portland - SE Lafayette
$PM_{2.5}$	160490002	45.93127	-116.116	RURAL	USFS COMPOUND ON EAST EDGE OF TOWN
$PM_{2.5}$	530330057	47.55975	-122.338	SUBURBAN	SEATTLE - DUWAMISH
$PM_{2.5}$	530670013	47.0294	-122.822	SUBURBAN	LACEY - COLLEGE ST
$PM_{2.5}$	410670004	45.5285	-122.972	SUBURBAN	Hillsboro - Hare Field
$PM_{2.5}$	530530031	47.2656	-122.386	SUBURBAN	TACOMA - ALEXANDER AVE
$PM_{2.5}$	160570005	46.72182	-116.96	RURAL	R&P 1400 PM2.5 TEOM. UNIVERSITY OF IDAHO PLANT SCIENCES SITE.
$PM_{2.5}$	160690012	46.40835	-116.993	SUBURBAN	SUNSET PARK LOCATION, BETWEEN CITY CENTER AND POTLACH CORP.,
$PM_{2.5}$	410650007	45.60242	-121.203	URBAN AND CENTER CITY	The Dalles - Cherry Drive
$PM_{2.5}$	530770016	46.37543	-120.729	RURAL	White Swan-Yakama Tribe
$PM_{2.5}$	530330024	47.755	-122.281	SUBURBAN	LAKE FOREST PARK TOWNE CENTER
$PM_{2.5}$	490494001	40.34139	-111.714	SUBURBAN	Lindon
$PM_{2.5}$	530750006	47.23136	-117.369	URBAN AND CENTER CITY	ROSALIA - JOSEPHINE ST
$PM_{2.5}$	530650002	47.88528	-117.989	SUBURBAN	SPOKANE - WELLPINIT FORD RD (SPOKANE TRIBE)
$PM_{2.5}$	410432002	44.3958	-122.731	RURAL	Sweet Home - FD (SFD)

$PM_{2.5}$	530611007	48.05432	-122.172	SUBURBAN	MARYSVILLE - 7TH AVE (Marysville Junior High)
$PM_{2.5}$	490490002	40.25361	-111.663	URBAN AND CENTER CITY	North Provo
$PM_{2.5}$	410010004	44.78822	-117.845	SUBURBAN	US FOREST SERVICE OFFICE - BAKER CITY
$PM_{2.5}$	410290133	42.31411	-122.879	URBAN AND CENTER CITY	Medford - Grant & Belmont Sts. (MGB)
$PM_{2.5}$	530750005	46.8153	-117.874	RURAL	LACAROSSE - HILL ST
$PM_{2.5}$	410130100	44.29979	-120.845	RURAL	Prineville - Davidson Park
$PM_{2.5}$	410190002	43.2266	-123.365	SUBURBAN	ROSEBURG, OR; BLM OFFICE - RGV
$PM_{2.5}$	530630021	47.67248	-117.365	URBAN AND CENTER CITY	SPOKANE - AUGUSTA AVE
$PM_{2.5}$	490030003	41.49271	-112.019	SUBURBAN	Brigham City
$PM_{2.5}$	410590121	45.65223	-118.823	SUBURBAN	Pendleton - McKay Creek
$PM_{2.5}$	530272002	46.97228	-123.832	SUBURBAN	ABERDEEN - DIVISION ST
$PM_{2.5}$	410250003	43.58925	-119.049	URBAN AND CENTER CITY	Burns - Washington Park (BWS)
$PM_{2.5}$	530530029	47.1864	-122.452	SUBURBAN	TACOMA - L STREET
$PM_{2.5}$	410430009	44.61569	-123.091	URBAN AND CENTER CITY	Albany - Caliapooia School
$PM_{2.5}$	530610020	48.2469	-121.603	URBAN AND CENTER CITY	DARRINGTON - FIR ST (Darrington High School)
$PM_{2.5}$	530331011	47.53091	-122.321	URBAN AND CENTER CITY	SEATTLE - SOUTH PARK #2
$PM_{2.5}$	530410004	46.66409	-122.967	URBAN AND CENTER CITY	CHEHALIS - MARKET BLVD
$PM_{2.5}$	530251002	47.1303	-119.274	URBAN AND CENTER CITY	MOSES LAKE - BALSAM ST
$PM_{2.5}$	160090011	47.33861	-116.886	RURAL	0
$PM_{2.5}$	410330114	42.43414	-123.348	SUBURBAN	GRANTS PASS PARKSIDE SCHOOL
$PM_{2.5}$	410330011	42.29009	-123.232	RURAL	PROVOLT, OR AT THE BLM SEED ORCHARD
$PM_{2.5}$	490570002	41.20632	-111.976	URBAN AND CENTER CITY	Ogden
$PM_{2.5}$	160790017	47.53639	-116.237	URBAN AND CENTER CITY	0
$PM_{2.5}$	530370002	46.99364	-120.545	URBAN AND CENTER CITY	ELLENSBURG - RUBY ST
$PM_{2.5}$	410330036	42.1617	-123.648	RURAL	Cave Junction - USFS Office (CJFS)
$PM_{2.5}$	530330037	47.61311	-122.202	SUBURBAN	BELLEVUE - BELLEVUE WAY NE

$PM_{2.5}$	410230002	44.418	-118.951	RURAL	John Day Dayton (JDD)
$PM_{2.5}$	160150001	43.82291	-115.84	RURAL	SITE IS AT SHERRIF'S OFFICE
$PM_{2.5}$	530090015	48.36606	-124.61	URBAN AND CENTER CITY	Neah Bay 2-Makah Tribe
$PM_{2.5}$	410290019	42.62323	-122.81	RURAL	SHADY COVE School (SCS)
$PM_{2.5}$	300490026	46.65876	-112.013	SUBURBAN	ROSSITER PUMP HOUSE
$PM_{2.5}$	530050002	46.21835	-119.204	URBAN AND CENTER CITY	KENNEWICK - METALINE
$PM_{2.5}$	530030004	46.42542	-117.06	SUBURBAN	CLARKSTON - 13TH ST
$PM_{2.5}$	530310003	48.12919	-122.779	SUBURBAN	Port Townsend-San Juan
$PM_{2.5}$	300530018	48.39155	-115.553	URBAN AND CENTER CITY	Libby Courthouse Annex
$PM_{2.5}$	530770009	46.59806	-120.499	URBAN AND CENTER CITY	YAKIMA - 4TH AVE
$PM_{2.5}$	530130002	46.318	-117.985	RURAL	DAYTON - W MAIN
$PM_{2.5}$	410170004	44.2921	-121.556	RURAL	Sisters Forest Service Station (SFS)
$PM_{2.5}$	490353006	40.73639	-111.872	SUBURBAN	Hawthorne
$PM_{2.5}$	530570015	48.4102	-122.338	SUBURBAN	MT VERNON - 2ND AVE
$PM_{2.5}$	530730015	48.76278	-122.44	SUBURBAN	BELLINGHAM - YEW STREET
$PM_{2.5}$	530470010	48.47724	-120.191	RURAL	WINTHROP - CHEWUCH RD
$PM_{2.5}$	160270002	43.58031	-116.563	URBAN AND CENTER CITY	SITE IS MIDWAY BETWEEN A MAJOR STREET AND A LOCAL STREET.
$PM_{2.5}$	530750003	46.72447	-117.18	SUBURBAN	PULLMAN - DEXTER AVE 4
$PM_{2.5}$	530770015	46.38024	-120.333	URBAN AND CENTER CITY	TOPPENISH - WARD RD (YAKAMA TRIBE)
$PM_{2.5}$	410392013	43.74435	-122.48	SUBURBAN	Oakridge - (OAK)
$PM_{2.5}$	160590004	45.1819	-113.89	RURAL	SALMON IDAHO, OPEN FIELD, GRASS COVERED AND PASTURE
$PM_{2.5}$	410370001	42.18922	-120.354	RURAL	Lakeview, CENTER & M ST. (LCM)
$PM_{2.5}$	530090013	48.29786	-124.625	RURAL	CHEEKA PEAK
$PM_{2.5}$	530470013	48.39999	-119.519	SUBURBAN	Omak-Colville Tribe
$PM_{2.5}$	530110022	45.8639	-122.411	RURAL	YACOLT - YACOLT RD
$PM_{2.5}$	160010010	43.6007	-116.348	URBAN AND CENTER CITY	St. Luke's Meridian
$PM_{2.5}$	410090004	45.76853	-122.772	RURAL	SAUVIE ISLAND-SIS

$PM_{2.5}$	410030013	44.5884	-123.267	SUBURBAN	NW CORNER OF ATHLETIC FIELD AT HIGHLAND VIEW INTERMEDIATE SCHOOL
$PM_{2.5}$	530332004	47.38611	-122.23	URBAN AND CENTER CITY	KENT - JAMES & CENTRAL
$PM_{2.5}$	530070010	47.59886	-120.665	SUBURBAN	LEAVENWORTH - EVANS ST
$PM_{2.5}$	530630047	47.69978	-117.426	URBAN AND CENTER CITY	SPOKANE - MONROE ST
$PM_{2.5}$	410630001	45.42635	-117.296	RURAL	Enterprise - USFS
$PM_{2.5}$	410670111	45.47019	-122.816	URBAN AND CENTER CITY	Beaverton - Highland Park
$PM_{2.5}$	530010003	47.12	-118.382	RURAL	RITZVILLE - ALDER ST
$PM_{2.5}$	530210002	46.5754	-119.002	RURAL	MESA - PEPOIT WAY
$PM_{2.5}$	410350004	42.1903	-121.731	SUBURBAN	Klamath Falls - Peterson School
$PM_{2.5}$	530710005	46.05881	-118.351	SUBURBAN	WALLA WALL - 12TH ST
$PM_{2.5}$	530450007	47.21355	-123.101	URBAN AND CENTER CITY	Shelton - W Franklin

S-Table 3. List of common AQS sites used and statistics per AIRPACT version.

Version	Species	Unit	AQSID	Forecast Mean	Observation Mean	FB [%]	FE [%]	RMSE	R^2 [-]
AP-3	O_3	ppb	530090013	36	36	0	15	7	0.46
AP-3	O_3	ppb	300298001	41	35	19	24	11	0.27
AP-3	O_3	ppb	490571003	57	54	5	12	9	0.4
AP-3	O_3	ppb	160010010	43	42	3	15	8	0.58
AP-3	O_3	ppb	410090004	38	33	15	22	10	0.46
AP-3	O_3	ppb	490490002	49	43	19	24	12	0.57
AP-3	O_3	ppb	530330017	41	35	19	25	11	0.45
AP-3	O_3	ppb	410050004	38	36	5	17	7	0.6
AP-3	O_3	ppb	490495010	60	54	10	14	10	0.26
AP-3	O_3	ppb	530630001	46	48	-4	10	6	0.55
AP-3	O_3	ppb	530530012	42	41	3	15	8	0.22
AP-3	O_3	ppb	410390060	41	35	16	21	10	0.56
AP-3	O_3	ppb	530330080	27	26	1	33	10	0.3
AP-3	O_3	ppb	410510080	32	29	12	27	9	0.53
AP-3	O_3	ppb	530330023	43	37	17	23	10	0.54
AP-3	O_3	ppb	490110004	57	47	20	22	13	0.55
AP-3	O_3	ppb	530110011	41	37	11	20	10	0.51
AP-3	O_3	ppb	490030003	57	54	6	12	8	0.39
AP-3	O_3	ppb	160010017	52	49	5	15	10	0.23
AP-3	O_3	ppb	410391007	42	36	17	21	10	0.54

AP-3	O_3	ppb	490353006	45	42	11	22	10	0.67
AP-3	O_3	ppb	160230101	48	46	5	12	7	0.36
AP-3	O_3	ppb	530730005	37	31	18	24	10	0.35
AP-3	O_3	ppb	490570002	48	42	18	24	11	0.63
AP-3	O_3	ppb	530330010	42	37	16	22	11	0.45
AP-4	O_3	ppb	530090013	36	37	-4	15	6	0.58
AP-4	O_3	ppb	300298001	43	35	23	27	12	0.26
AP-4	O_3	ppb	490571003	52	47	11	17	11	0.54
AP-4	O_3	ppb	160010010	44	37	20	26	12	0.5
AP-4	O_3	ppb	410090004	39	35	9	23	12	0.46
AP-4	O_3	ppb	490490002	51	43	22	25	14	0.55
AP-4	O_3	ppb	530330017	45	36	20	26	14	0.45
AP-4	O_3	ppb	410050004	43	41	1	20	11	0.59
AP-4	O_3	ppb	490495010	53	45	19	22	12	0.55
AP-4	O_3	ppb	530630001	46	46	0	16	10	0.2
AP-4	O_3	ppb	530530012	49	42	14	19	14	0.06
AP-4	O_3	ppb	410390060	39	37	4	19	10	0.52
AP-4	O_3	ppb	530330080	26	27	-8	35	9	0.51
AP-4	O_3	ppb	410510080	35	29	18	29	10	0.56
AP-4	O_3	ppb	530330023	48	39	17	24	14	0.57
AP-4	O_3	ppb	490110004	49	40	25	27	13	0.64
AP-4	O_3	ppb	530110011	40	36	4	23	11	0.56
AP-4	O_3	ppb	490030003	55	49	12	17	12	0.3
AP-4	O_3	ppb	160010017	51	47	7	23	16	0.06
AP-4	O_3	ppb	410391007	43	39	10	20	11	0.51
AP-4	O_3	ppb	490353006	46	42	9	20	11	0.71
AP-4	O_3	ppb	160230101	49	44	11	16	11	0.19
AP-4	O_3	ppb	530730005	39	31	17	26	13	0.33
AP-4	O_3	ppb	490570002	50	43	18	22	11	0.62
AP-4	O_3	ppb	530330010	40	35	13	24	13	0.46
AP-5	O_3	ppb	530090013	34	36	-8	16	7	0.54
AP-5	O_3	ppb	300298001	42	36	17	22	12	0.19
AP-5	O_3	ppb	490571003	50	47	10	19	11	0.49
AP-5	O_3	ppb	160010010	41	40	6	18	10	0.46
AP-5	O_3	ppb	410090004	35	34	1	17	9	0.46
AP-5	O_3	ppb	490490002	51	43	21	24	13	0.54
AP-5	O_3	ppb	530330017	39	36	9	20	12	0.35
AP-5	O_3	ppb	410050004	37	38	-5	16	7	0.56
AP-5	O_3	ppb	490495010	50	46	10	17	13	0.3
AP-5	O_3	ppb	530630001	44	44	-2	15	15	0.16
AP-5	O_3	ppb	530530012	46	43	6	14	9	0.23
AP-5	O_3	ppb	410390060	36	37	-2	17	8	0.52
AP-5	O_3	ppb	530330080	27	29	-9	25	8	0.5

AP-5	O_3	ppb	410510080	35	32	12	23	9	0.45
AP-5	O_3	ppb	530330023	41	40	5	19	12	0.44
AP-5	O_3	ppb	490110004	50	45	14	19	11	0.56
AP-5	O_3	ppb	530110011	37	36	1	17	9	0.53
AP-5	O_3	ppb	490030003	51	43	19	24	13	0.35
AP-5	O_3	ppb	160010017	48	47	5	21	13	0.14
AP-5	O_3	ppb	410391007	38	37	5	18	9	0.44
AP-5	O_3	ppb	490353006	48	45	8	17	11	0.58
AP-5	O_3	ppb	160230101	47	45	6	14	10	0.16
AP-5	O_3	ppb	530730005	36	34	4	20	12	0.18
AP-5	O_3	ppb	490570002	48	46	10	20	11	0.56
AP-5	O_3	ppb	530330010	34	36	-6	22	13	0.27
AP-3	$PM_{2.5}$	µg m^{-3}	530150015	6	5.1	7	49	5	0.28
AP-3	$PM_{2.5}$	µg m^{-3}	410610119	3.8	7.4	-60	69	7	0.12
AP-3	$PM_{2.5}$	µg m^{-3}	530610005	13	6	82	85	9	0.27
AP-3	$PM_{2.5}$	µg m^{-3}	160090010	4.6	10	-76	80	6	0
AP-3	$PM_{2.5}$	µg m^{-3}	410170120	5.5	5.3	0	43	5	0.36
AP-3	$PM_{2.5}$	µg m^{-3}	530470009	2.7	9.2	-101	103	9	0.2
AP-3	$PM_{2.5}$	µg m^{-3}	530531018	11	6.9	39	57	8	0.35
AP-3	$PM_{2.5}$	µg m^{-3}	530330017	5.7	5.4	1	36	3	0.43
AP-3	$PM_{2.5}$	µg m^{-3}	410050004	10	5	46	53	2	0.01
AP-3	$PM_{2.5}$	µg m^{-3}	410470041	7.8	6.4	12	40	5	0.47
AP-3	$PM_{2.5}$	µg m^{-3}	410390060	7.3	6.5	9	41	7	0.22
AP-3	$PM_{2.5}$	µg m^{-3}	530330080	15	6.2	76	78	12	0.33
AP-3	$PM_{2.5}$	µg m^{-3}	410510080	15	7.5	61	66	11	0.48
AP-3	$PM_{2.5}$	µg m^{-3}	160490002	4.4	4.1	37	64	7	0.51
AP-3	$PM_{2.5}$	µg m^{-3}	530330057	15	10	42	52	9	0.3
AP-3	$PM_{2.5}$	µg m^{-3}	530670013	7.1	5.9	10	51	6	0.38
AP-3	$PM_{2.5}$	µg m^{-3}	410670004	9.2	7.3	20	45	6	0.42
AP-3	$PM_{2.5}$	µg m^{-3}	530530031	15	7.4	60	65	11	0.43
AP-3	$PM_{2.5}$	µg m^{-3}	160570005	6	4.4	49	68	5	0.4
AP-3	$PM_{2.5}$	µg m^{-3}	160690012	7	5.7	31	49	5	0.38
AP-3	$PM_{2.5}$	µg m^{-3}	410650007	5.1	6.2	-21	45	4	0.25
AP-3	$PM_{2.5}$	µg m^{-3}	530770016	5	6.4	-28	45	3	0.33
AP-3	$PM_{2.5}$	µg m^{-3}	530330024	13	7.4	55	63	9	0.39
AP-3	$PM_{2.5}$	µg m^{-3}	490494001	5.6	9.2	-43	60	7	0.07
AP-3	$PM_{2.5}$	µg m^{-3}	530750006	5.2	4.6	5	44	3	0.24
AP-3	$PM_{2.5}$	µg m^{-3}	530650002	4.7	5.1	-19	45	3	0.29
AP-3	$PM_{2.5}$	µg m^{-3}	410432002	4.9	7.1	-35	78	8	0.01
AP-3	$PM_{2.5}$	µg m^{-3}	530611007	9.3	7.7	22	50	6	0.16
AP-3	$PM_{2.5}$	µg m^{-3}	490490002	5.5	6.6	-14	53	4	0.11
AP-3	$PM_{2.5}$	µg m^{-3}	410010004	3.9	7.5	-68	73	5	0.18
AP-3	$PM_{2.5}$	µg m^{-3}	410290133	5.9	9	-33	67	8	0.03

AP-3	$PM_{2.5}$	μg m^{-3}	530750005	4.9	4.2	9	46	3	0.4
AP-3	$PM_{2.5}$	μg m^{-3}	410130100	3.3	7.9	-66	77	8	0.02
AP-3	$PM_{2.5}$	μg m^{-3}	410190002	5	6.3	-36	55	6	0.11
AP-3	$PM_{2.5}$	μg m^{-3}	530630021	8.9	8.8	-6	33	4	0.36
AP-3	$PM_{2.5}$	μg m^{-3}	490030003	5.2	8.1	-34	57	6	0.26
AP-3	$PM_{2.5}$	μg m^{-3}	410590121	4.1	7.4	-54	62	6	0.18
AP-3	$PM_{2.5}$	μg m^{-3}	530272002	4.2	3.9	-13	54	4	0.23
AP-3	$PM_{2.5}$	μg m^{-3}	410250003	2.6	9.8	-100	103	8	0.02
AP-3	$PM_{2.5}$	μg m^{-3}	530530029	13	7.9	52	60	8	0.42
AP-3	$PM_{2.5}$	μg m^{-3}	410430009	7.6	6.1	15	45	6	0.34
AP-3	$PM_{2.5}$	μg m^{-3}	530610020	3.6	7.3	-47	75	7	0.04
AP-3	$PM_{2.5}$	μg m^{-3}	530331011	15	8.5	48	55	10	0.39
AP-3	$PM_{2.5}$	μg m^{-3}	530410004	6.1	5.7	-24	55	4	0.37
AP-3	$PM_{2.5}$	μg m^{-3}	530251002	5.2	6.1	-23	43	4	0.42
AP-3	$PM_{2.5}$	μg m^{-3}	160090011	4.9	7	-38	51	5	0.28
AP-3	$PM_{2.5}$	μg m^{-3}	410330114	5.1	7	-32	57	6	0.17
AP-3	$PM_{2.5}$	μg m^{-3}	410330011	3.9	5.3	-44	64	4	0.1
AP-3	$PM_{2.5}$	μg m^{-3}	490570002	8.5	11	-14	45	7	0.2
AP-3	$PM_{2.5}$	μg m^{-3}	160790017	4.8	13	-74	86	12	0.02
AP-3	$PM_{2.5}$	μg m^{-3}	530370002	4.9	7.8	-23	51	9	0.39
AP-3	$PM_{2.5}$	μg m^{-3}	410330036	3.3	6	-73	89	4	0.04
AP-3	$PM_{2.5}$	μg m^{-3}	530330037	12	4.7	81	83	10	0.34
AP-3	$PM_{2.5}$	μg m^{-3}	410230002	3.2	8.9	-93	102	7	0
AP-3	$PM_{2.5}$	μg m^{-3}	160150001	4	5.7	-37	57	2	0
AP-3	$PM_{2.5}$	μg m^{-3}	530090015	1.9	3.5	-81	88	2	0.12
AP-3	$PM_{2.5}$	μg m^{-3}	410290019	4.2	5.4	-34	54	5	0.08
AP-3	$PM_{2.5}$	μg m^{-3}	300490026	5.8	9	-17	49	6	0.23
AP-3	$PM_{2.5}$	μg m^{-3}	530050002	5.6	6.2	-17	40	3	0.46
AP-3	$PM_{2.5}$	μg m^{-3}	530030004	5.4	8.1	-35	48	6	0.45
AP-3	$PM_{2.5}$	μg m^{-3}	530310003	5.3	5.4	-11	42	3	0.25
AP-3	$PM_{2.5}$	μg m^{-3}	300530018	4.9	11	-69	77	9	0.04
AP-3	$PM_{2.5}$	μg m^{-3}	530770009	5.7	8.6	-24	49	7	0.34
AP-3	$PM_{2.5}$	μg m^{-3}	530130002	3.8	5.3	-36	47	3	0.32
AP-3	$PM_{2.5}$	μg m^{-3}	410170004	4.9	11	-77	84	35	0.42
AP-3	$PM_{2.5}$	μg m^{-3}	490353006	11	9.2	35	60	8	0.2
AP-3	$PM_{2.5}$	μg m^{-3}	530570015	6.1	4.6	18	44	4	0.28
AP-3	$PM_{2.5}$	μg m^{-3}	530730015	6.6	5.7	11	42	4	0.25
AP-3	$PM_{2.5}$	μg m^{-3}	530470010	2.7	7.6	-91	92	7	0.21
AP-3	$PM_{2.5}$	μg m^{-3}	160270002	15.3	10	19	36	2	0.01
AP-3	$PM_{2.5}$	μg m^{-3}	530750003	5.5	5.6	-4	39	3	0.47
AP-3	$PM_{2.5}$	μg m^{-3}	530770015	5.8	8.5	-22	46	6	0.52
AP-3	$PM_{2.5}$	μg m^{-3}	410392013	3.8	9.3	-79	97	11	0
AP-3	$PM_{2.5}$	μg m^{-3}	160590004	5	14	-67	84	18	0.48

AP-3	$PM_{2.5}$	$\mu g\ m^{-3}$	410370001	2.5	8.6	-86	90	11	0.02
AP-3	$PM_{2.5}$	$\mu g\ m^{-3}$	530090013	1.7	2.3	-47	65	2	0.19
AP-3	$PM_{2.5}$	$\mu g\ m^{-3}$	530470013	4	7.6	-61	65	5	0.28
AP-3	$PM_{2.5}$	$\mu g\ m^{-3}$	530110022	5.3	4.4	18	50	4	0.17
AP-3	$PM_{2.5}$	$\mu g\ m^{-3}$	160010010	23	14	34	48	6	0.05
AP-3	$PM_{2.5}$	$\mu g\ m^{-3}$	410090004	7.4	5.5	17	42	5	0.42
AP-3	$PM_{2.5}$	$\mu g\ m^{-3}$	410030013	5.3	5.2	-16	48	5	0.38
AP-3	$PM_{2.5}$	$\mu g\ m^{-3}$	530332004	12	7.9	44	60	8	0.24
AP-3	$PM_{2.5}$	$\mu g\ m^{-3}$	530070010	3.3	6.9	-58	71	8	0.42
AP-3	$PM_{2.5}$	$\mu g\ m^{-3}$	530630047	8.6	6.8	26	42	5	0.47
AP-3	$PM_{2.5}$	$\mu g\ m^{-3}$	410630001	2.6	6	-78	81	5	0.1
AP-3	$PM_{2.5}$	$\mu g\ m^{-3}$	410670111	11.9	5.8	63	67	9	0.51
AP-3	$PM_{2.5}$	$\mu g\ m^{-3}$	530010003	4.6	5.2	-19	43	3	0.38
AP-3	$PM_{2.5}$	$\mu g\ m^{-3}$	530210002	5.5	5.8	-13	41	4	0.39
AP-3	$PM_{2.5}$	$\mu g\ m^{-3}$	410350004	5.4	10.3	-43	70	11	0.06
AP-3	$PM_{2.5}$	$\mu g\ m^{-3}$	530710005	5.5	6.2	-16	42	4	0.42
AP-3	$PM_{2.5}$	$\mu g\ m^{-3}$	530450007	5.1	7.3	-50	62	3	0.29
AP-4	$PM_{2.5}$	$\mu g\ m^{-3}$	530150015	7.1	6.3	7	36	5	0.35
AP-4	$PM_{2.5}$	$\mu g\ m^{-3}$	410610119	3.5	9.1	-70	73	9	0.36
AP-4	$PM_{2.5}$	$\mu g\ m^{-3}$	530610005	8.7	6.4	37	55	4	0.18
AP-4	$PM_{2.5}$	$\mu g\ m^{-3}$	160090010	2.7	13	-122	123	12	0.17
AP-4	$PM_{2.5}$	$\mu g\ m^{-3}$	410170120	8.6	6	43	58	7	0.13
AP-4	$PM_{2.5}$	$\mu g\ m^{-3}$	530470009	2.1	9.4	-120	121	12	0.38
AP-4	$PM_{2.5}$	$\mu g\ m^{-3}$	530531018	10	6.5	43	59	8	0.42
AP-4	$PM_{2.5}$	$\mu g\ m^{-3}$	530330017	5.7	5.3	4	51	4	0.13
AP-4	$PM_{2.5}$	$\mu g\ m^{-3}$	410050004	10	5.2	45	63	4	0
AP-4	$PM_{2.5}$	$\mu g\ m^{-3}$	410470041	15	7.2	67	70	12	0.38
AP-4	$PM_{2.5}$	$\mu g\ m^{-3}$	410390060	11	7.9	34	48	9	0.34
AP-4	$PM_{2.5}$	$\mu g\ m^{-3}$	530330080	12	6.4	49	59	9	0.25
AP-4	$PM_{2.5}$	$\mu g\ m^{-3}$	410510080	16	7.5	65	69	14	0.39
AP-4	$PM_{2.5}$	$\mu g\ m^{-3}$	160490002	2.1	7.6	-17	86	11	0.15
AP-4	$PM_{2.5}$	$\mu g\ m^{-3}$	530330057	14	10.3	-10	32	1	0
AP-4	$PM_{2.5}$	$\mu g\ m^{-3}$	530670013	8	7.2	6	39	5	0.54
AP-4	$PM_{2.5}$	$\mu g\ m^{-3}$	410670004	14	7.1	57	63	12	0.42
AP-4	$PM_{2.5}$	$\mu g\ m^{-3}$	530530031	11	8	18	42	8	0.47
AP-4	$PM_{2.5}$	$\mu g\ m^{-3}$	160570005	4.2	6	50	99	8	0.02
AP-4	$PM_{2.5}$	$\mu g\ m^{-3}$	160690012	4.9	8.3	7	69	11	0.02
AP-4	$PM_{2.5}$	$\mu g\ m^{-3}$	410650007	6.3	6.8	-14	45	6	0.16
AP-4	$PM_{2.5}$	$\mu g\ m^{-3}$	530770016	4.1	6.3	-51	69	6	0.15
AP-4	$PM_{2.5}$	$\mu g\ m^{-3}$	530330024	9.5	7.8	17	42	6	0.46
AP-4	$PM_{2.5}$	$\mu g\ m^{-3}$	490494001	7.2	9.5	-5	56	11	0.15
AP-4	$PM_{2.5}$	$\mu g\ m^{-3}$	530750006	3.5	5.4	-36	58	5	0.08
AP-4	$PM_{2.5}$	$\mu g\ m^{-3}$	530650002	2.6	5.9	-74	88	6	0.3

AP-4	$PM_{2.5}$	µg m^{-3}	410432002	8.2	6.2	24	54	14	0.06
AP-4	$PM_{2.5}$	µg m^{-3}	530611007	9.2	7.9	17	46	4	0.13
AP-4	$PM_{2.5}$	µg m^{-3}	490490002	7.3	7.3	1	43	5	0.26
AP-4	$PM_{2.5}$	µg m^{-3}	410010004	4.5	8	-53	58	7	0.16
AP-4	$PM_{2.5}$	µg m^{-3}	410290133	16	12	36	57	12	0.29
AP-4	$PM_{2.5}$	µg m^{-3}	530750005	3.7	5.3	-28	57	6	0.07
AP-4	$PM_{2.5}$	µg m^{-3}	410130100	4.9	9.8	-39	58	11	0.13
AP-4	$PM_{2.5}$	µg m^{-3}	410190002	8.6	6.8	16	46	6	0.3
AP-4	$PM_{2.5}$	µg m^{-3}	530630021	5.9	9.3	-57	68	5	0.11
AP-4	$PM_{2.5}$	µg m^{-3}	490030003	3.6	6.9	-38	59	7	0.44
AP-4	$PM_{2.5}$	µg m^{-3}	410590121	7.6	7.3	3	48	6	0.28
AP-4	$PM_{2.5}$	µg m^{-3}	530272002	3.8	5.7	-44	52	3	0.27
AP-4	$PM_{2.5}$	µg m^{-3}	410250003	2.6	9.2	-99	100	9	0.39
AP-4	$PM_{2.5}$	µg m^{-3}	530530029	9.1	7.9	11	37	6	0.44
AP-4	$PM_{2.5}$	µg m^{-3}	410430009	12	7.1	51	58	10	0.32
AP-4	$PM_{2.5}$	µg m^{-3}	530610020	3.1	6.5	-47	64	5	0.08
AP-4	$PM_{2.5}$	µg m^{-3}	530331011	14	9.4	28	40	9	0.45
AP-4	$PM_{2.5}$	µg m^{-3}	530410004	6.6	6.6	-16	44	4	0.43
AP-4	$PM_{2.5}$	µg m^{-3}	530251002	4.3	6.8	-48	60	5	0.2
AP-4	$PM_{2.5}$	µg m^{-3}	160090011	2.8	7.8	-86	90	8	0.07
AP-4	$PM_{2.5}$	µg m^{-3}	410330114	13	8.9	34	52	24	0.35
AP-4	$PM_{2.5}$	µg m^{-3}	410330011	5.6	7.1	-31	49	13	0.31
AP-4	$PM_{2.5}$	µg m^{-3}	490570002	9.2	12	-24	44	8	0.29
AP-4	$PM_{2.5}$	µg m^{-3}	160790017	2.4	14	-126	128	16	0.21
AP-4	$PM_{2.5}$	µg m^{-3}	530370002	3.5	6.5	-50	62	6	0.32
AP-4	$PM_{2.5}$	µg m^{-3}	410330036	5.7	9.1	-39	51	14	0.24
AP-4	$PM_{2.5}$	µg m^{-3}	530330037	9.1	5.2	46	54	6	0.29
AP-4	$PM_{2.5}$	µg m^{-3}	410230002	2.2	10	-113	113	11	0.25
AP-4	$PM_{2.5}$	µg m^{-3}	160150001	2.5	5.7	-63	84	4	0
AP-4	$PM_{2.5}$	µg m^{-3}	530090015	2.4	4.1	-59	65	3	0.06
AP-4	$PM_{2.5}$	µg m^{-3}	410290019	5.7	8.1	-9	40	15	0.13
AP-4	$PM_{2.5}$	µg m^{-3}	300490026	3.1	8.3	-79	83	9	0.21
AP-4	$PM_{2.5}$	µg m^{-3}	530050002	5	6.5	-35	54	5	0.29
AP-4	$PM_{2.5}$	µg m^{-3}	530030004	3.3	8.4	-81	83	7	0.16
AP-4	$PM_{2.5}$	µg m^{-3}	530310003	5.4	5.9	-21	41	5	0.16
AP-4	$PM_{2.5}$	µg m^{-3}	300530018	3.8	12	-78	86	13	0.32
AP-4	$PM_{2.5}$	µg m^{-3}	530770009	5.5	9.5	-59	69	7	0.37
AP-4	$PM_{2.5}$	µg m^{-3}	530130002	4	5.1	-24	46	3	0.24
AP-4	$PM_{2.5}$	µg m^{-3}	410170004	4.8	5.2	-4	49	5	0.05
AP-4	$PM_{2.5}$	µg m^{-3}	490353006	13	8.5	52	62	9	0.47
AP-4	$PM_{2.5}$	µg m^{-3}	530570015	5.4	4.6	9	40	4	0.21
AP-4	$PM_{2.5}$	µg m^{-3}	530730015	5.6	7	-23	46	4	0.25
AP-4	$PM_{2.5}$	µg m^{-3}	530470010	1.8	6.8	-116	116	6	0.22

AP-4	$PM_{2.5}$	µg m^{-3}	160270002	9.5	8.3	9	58	5	0
AP-4	$PM_{2.5}$	µg m^{-3}	530750003	3.8	5.5	-32	52	4	0.05
AP-4	$PM_{2.5}$	µg m^{-3}	530770015	5.6	11	-53	65	10	0.3
AP-4	$PM_{2.5}$	µg m^{-3}	410392013	6	9.6	-43	61	15	0.05
AP-4	$PM_{2.5}$	µg m^{-3}	160590004	2.4	13	-121	122	17	0.16
AP-4	$PM_{2.5}$	µg m^{-3}	410370001	1.9	10	-110	110	16	0.22
AP-4	$PM_{2.5}$	µg m^{-3}	530090013	2.3	2.3	-4	43	2	0.07
AP-4	$PM_{2.5}$	µg m^{-3}	530470013	2.7	13	-111	112	27	0.55
AP-4	$PM_{2.5}$	µg m^{-3}	530110022	4.5	6	-22	50	5	0.09
AP-4	$PM_{2.5}$	µg m^{-3}	160010010	7.4	6.7	1	53	4	0.01
AP-4	$PM_{2.5}$	µg m^{-3}	410090004	8.3	5.7	29	44	6	0.33
AP-4	$PM_{2.5}$	µg m^{-3}	410030013	9	5.8	42	52	7	0.36
AP-4	$PM_{2.5}$	µg m^{-3}	530332004	9.8	6.8	35	53	7	0.38
AP-4	$PM_{2.5}$	µg m^{-3}	530070010	2.9	8.4	-93	94	8	0.26
AP-4	$PM_{2.5}$	µg m^{-3}	530630047	6.6	8	-14	41	6	0.21
AP-4	$PM_{2.5}$	µg m^{-3}	410630001	2.7	6.9	-69	71	8	0.2
AP-4	$PM_{2.5}$	µg m^{-3}	410670111	15	6	79	82	13	0.39
AP-4	$PM_{2.5}$	µg m^{-3}	530010003	3.9	5.3	-27	53	5	0.05
AP-4	$PM_{2.5}$	µg m^{-3}	530210002	4.7	6.3	-36	57	5	0.19
AP-4	$PM_{2.5}$	µg m^{-3}	410350004	5.9	11	-36	55	11	0.28
AP-4	$PM_{2.5}$	µg m^{-3}	530710005	6	6	-2	50	5	0.2
AP-4	$PM_{2.5}$	µg m^{-3}	530450007	5.3	6.5	-30	48	4	0.41
AP-5	$PM_{2.5}$	µg m^{-3}	530150015	6	5.5	-9	38	4	0.22
AP-5	$PM_{2.5}$	µg m^{-3}	410610119	2.7	5.9	-72	74	4	0.37
AP-5	$PM_{2.5}$	µg m^{-3}	530610005	9.2	4.7	60	77	8	0.22
AP-5	$PM_{2.5}$	µg m^{-3}	160090010	4.2	12	-107	111	12	0.56
AP-5	$PM_{2.5}$	µg m^{-3}	410170120	8.1	7.3	26	43	6	0.73
AP-5	$PM_{2.5}$	µg m^{-3}	530470009	3.5	9.6	-122	124	11	0.26
AP-5	$PM_{2.5}$	µg m^{-3}	530531018	8.9	5.6	35	60	9	0.15
AP-5	$PM_{2.5}$	µg m^{-3}	530330017	4.4	4	10	60	8	0.46
AP-5	$PM_{2.5}$	µg m^{-3}	410470041	8.7	5.8	28	46	5	0.3
AP-5	$PM_{2.5}$	µg m^{-3}	410390060	9	6.5	17	55	7	0.31
AP-5	$PM_{2.5}$	µg m^{-3}	530330080	11	5.9	48	60	9	0.16
AP-5	$PM_{2.5}$	µg m^{-3}	410510080	9.5	6.2	36	49	6	0.24
AP-5	$PM_{2.5}$	µg m^{-3}	160490002	3.5	5.7	-71	85	5	0.77
AP-5	$PM_{2.5}$	µg m^{-3}	530330057	11	7.8	16	49	7	0.18
AP-5	$PM_{2.5}$	µg m^{-3}	530670013	8.2	5.6	11	52	6	0.23
AP-5	$PM_{2.5}$	µg m^{-3}	410670004	9.2	6.5	25	43	7	0.3
AP-5	$PM_{2.5}$	µg m^{-3}	530530031	9	6.5	8	52	7	0.2
AP-5	$PM_{2.5}$	µg m^{-3}	160570005	5.6	4.3	37	83	7	0.79
AP-5	$PM_{2.5}$	µg m^{-3}	160690012	6.8	8.1	-6	61	8	0.72
AP-5	$PM_{2.5}$	µg m^{-3}	410650007	6	8.3	-39	55	8	0.54
AP-5	$PM_{2.5}$	µg m^{-3}	530770016	4.8	5.4	-36	72	8	0.64

AP-5	$PM_{2.5}$	μg m^{-3}	530330024	9.8	6.4	68	71	2	0.06
AP-5	$PM_{2.5}$	μg m^{-3}	490494001	7.3	6.4	-17	57	23	0.02
AP-5	$PM_{2.5}$	μg m^{-3}	530750006	3.9	5.3	-61	75	10	0.75
AP-5	$PM_{2.5}$	μg m^{-3}	530650002	3.5	5.9	-83	87	9	0.61
AP-5	$PM_{2.5}$	μg m^{-3}	410432002	4.9	7.1	-53	64	7	0.32
AP-5	$PM_{2.5}$	μg m^{-3}	530611007	8.4	6.8	10	54	6	0.22
AP-5	$PM_{2.5}$	μg m^{-3}	490490002	4.8	5.4	6	63	4	0.23
AP-5	$PM_{2.5}$	μg m^{-3}	410010004	4.2	7.3	-63	67	4	0.55
AP-5	$PM_{2.5}$	μg m^{-3}	410290133	10	10	15	47	11	0.66
AP-5	$PM_{2.5}$	μg m^{-3}	530750005	4	4.8	-46	67	10	0.75
AP-5	$PM_{2.5}$	μg m^{-3}	410130100	5.2	9.1	-54	59	7	0.57
AP-5	$PM_{2.5}$	μg m^{-3}	410190002	5.7	6.8	-35	48	5	0.26
AP-5	$PM_{2.5}$	μg m^{-3}	530630021	7.8	8.6	-21	57	9	0.74
AP-5	$PM_{2.5}$	μg m^{-3}	490030003	3.4	7.9	-94	98	6	0.22
AP-5	$PM_{2.5}$	μg m^{-3}	410590121	5.8	7.2	-24	43	6	0.73
AP-5	$PM_{2.5}$	μg m^{-3}	530272002	3.1	5.1	-64	69	4	0.1
AP-5	$PM_{2.5}$	μg m^{-3}	410250003	3	9.2	-105	107	8	0.28
AP-5	$PM_{2.5}$	μg m^{-3}	530530029	8.3	6.4	12	44	6	0.32
AP-5	$PM_{2.5}$	μg m^{-3}	410430009	8.4	6.1	21	44	6	0.25
AP-5	$PM_{2.5}$	μg m^{-3}	530610020	3.2	6.5	-40	81	9	0.17
AP-5	$PM_{2.5}$	μg m^{-3}	530331011	9.7	8.3	-8	46	7	0.15
AP-5	$PM_{2.5}$	μg m^{-3}	530410004	5.5	5.7	-33	52	5	0.16
AP-5	$PM_{2.5}$	μg m^{-3}	530251002	5	6.2	-47	65	10	0.61
AP-5	$PM_{2.5}$	μg m^{-3}	160090011	3.8	7.8	-98	106	5	0
AP-5	$PM_{2.5}$	μg m^{-3}	410330114	9.2	9.4	10	53	10	0.38
AP-5	$PM_{2.5}$	μg m^{-3}	410330011	4.6	8.3	-86	89	10	0.55
AP-5	$PM_{2.5}$	μg m^{-3}	490570002	5.8	7.5	-42	64	6	0.1
AP-5	$PM_{2.5}$	μg m^{-3}	160790017	3.9	13	-116	119	12	0.61
AP-5	$PM_{2.5}$	μg m^{-3}	530370002	5	7.6	-47	70	7	0.67
AP-5	$PM_{2.5}$	μg m^{-3}	410330036	7	9.3	-101	103	8	0.11
AP-5	$PM_{2.5}$	μg m^{-3}	530330037	10	3.5	84	86	7	0.08
AP-5	$PM_{2.5}$	μg m^{-3}	410230002	2.6	8.8	-117	119	8	0.36
AP-5	$PM_{2.5}$	μg m^{-3}	160150001	2.8	7.1	-103	117	7	0.03
AP-5	$PM_{2.5}$	μg m^{-3}	530090015	2.3	3.7	-58	67	3	0.03
AP-5	$PM_{2.5}$	μg m^{-3}	410290019	5.5	7.4	-69	72	6	0.43
AP-5	$PM_{2.5}$	μg m^{-3}	300490026	4.3	9.1	-68	76	9	0.36
AP-5	$PM_{2.5}$	μg m^{-3}	530050002	5.9	6.6	-38	57	10	0.66
AP-5	$PM_{2.5}$	μg m^{-3}	530030004	4.4	8.7	-83	87	9	0.75
AP-5	$PM_{2.5}$	μg m^{-3}	530310003	4.5	5.1	-35	53	3	0.25
AP-5	$PM_{2.5}$	μg m^{-3}	300530018	5.5	12	-91	95	13	0.44
AP-5	$PM_{2.5}$	μg m^{-3}	530770009	7.4	8.7	14	93	7	0.71
AP-5	$PM_{2.5}$	μg m^{-3}	530130002	3.8	5.7	-54	72	8	0.62
AP-5	$PM_{2.5}$	μg m^{-3}	410170004	4.8	10	-60	71	17	0.52

AP-5	$PM_{2.5}$	μg m^{-3}	490353006	8.9	8	-7	52	8	0.24
AP-5	$PM_{2.5}$	μg m^{-3}	530570015	5.2	3.2	39	51	4	0.19
AP-5	$PM_{2.5}$	μg m^{-3}	530730015	5.8	5.1	20	46	5	0.27
AP-5	$PM_{2.5}$	μg m^{-3}	530470010	3.4	7.7	-109	114	9	0.34
AP-5	$PM_{2.5}$	μg m^{-3}	160270002	13	9.7	17	56	9	0.4
AP-5	$PM_{2.5}$	μg m^{-3}	530750003	4.3	4.6	-25	56	8	0.86
AP-5	$PM_{2.5}$	μg m^{-3}	530770015	6.3	10.8	-71	77	9	0.64
AP-5	$PM_{2.5}$	μg m^{-3}	410392013	3.5	8.9	-100	102	9	0.6
AP-5	$PM_{2.5}$	μg m^{-3}	160590004	2.8	12	-121	134	14	0.22
AP-5	$PM_{2.5}$	μg m^{-3}	410370001	2.6	7.8	-108	109	8	0.07
AP-5	$PM_{2.5}$	μg m^{-3}	530090013	2.2	2.6	-3	45	6	0.02
AP-5	$PM_{2.5}$	μg m^{-3}	530470013	3.9	8.9	-83	101	10	0.34
AP-5	$PM_{2.5}$	μg m^{-3}	530110022	3.5	5	-44	61	6	0.28
AP-5	$PM_{2.5}$	μg m^{-3}	160010010	11	7.4	35	65	7	0.47
AP-5	$PM_{2.5}$	μg m^{-3}	410090004	6.5	5.1	3	49	5	0.17
AP-5	$PM_{2.5}$	μg m^{-3}	410030013	7.1	5.5	20	48	4	0.18
AP-5	$PM_{2.5}$	μg m^{-3}	530332004	8.3	6.3	19	54	6	0.25
AP-5	$PM_{2.5}$	μg m^{-3}	530070010	3.6	5.9	-74	80	5	0.14
AP-5	$PM_{2.5}$	μg m^{-3}	530630047	8.2	7.4	0	48	9	0.74
AP-5	$PM_{2.5}$	μg m^{-3}	410630001	2.9	6.8	-86	89	5	0.58
AP-5	$PM_{2.5}$	μg m^{-3}	410670111	10	5.3	54	62	8	0.22
AP-5	$PM_{2.5}$	μg m^{-3}	530010003	4.3	4.8	-38	59	10	0.74
AP-5	$PM_{2.5}$	μg m^{-3}	530210002	5.1	5.6	-43	65	11	0.67
AP-5	$PM_{2.5}$	μg m^{-3}	410350004	6.8	11	-57	63	7	0.54
AP-5	$PM_{2.5}$	μg m^{-3}	530710005	6	6.3	-16	51	8	0.71
AP-5	$PM_{2.5}$	μg m^{-3}	530450007	4.2	5.7	-48	56	4	0.26

S-Table 4. Seasonal evaluation results. Note that O_3 is based on total 26 AQS sites and for PM2.5, total 89 sites.

species	season	version	Forecast Mean [ppb or μg m^{-3}]	Observation Mean [ppb or μg m^{-3}]	MB [ppb or μg m^{-3}]	ME [ppb or μg m^{-3}]	FB [%]	FE [%]	NMB [%]	NME [%]	RMSE [ppb or μg m^{-3}]	R^2 [-]
O3	Spring	AP3	43	42	0.6	1.6	1.4	3.8	1.3	3.8	2.1	0.73
		AP4	48	43	5.5	5.7	12.1	12.5	12.9	13.4	6.7	0.43
		AP5	46	42	3.5	3.8	8.3	8.8	8.4	9.0	4.4	0.51
	Summer	AP3	45	41	3.5	3.8	8.3	9.1	8.6	9.4	4.4	0.73
		AP4	47	45	2.2	3.2	4.8	7.1	4.8	7.1	4.1	0.55
		AP5	42	45	-2.1	2.7	-4.5	6.4	-4.7	6.1	3.3	0.76
	Fall	AP3	38	31	7.8	7.8	23.4	23.4	25.3	25.3	8.1	0.87
		AP4	38	32	5.7	5.8	17.2	17.3	18.1	18.2	6.4	0.72
		AP5	37	32	4.4	4.7	13.2	13.9	13.6	14.4	5.9	0.57
	Winter	AP3	33	26	7.4	7.4	26.2	26.2	28.7	28.7	7.8	0.76
		AP4	32	26	7.0	7.0	25.5	25.5	27.2	27.2	7.8	0.58
		AP5	34	28	5.1	5.2	17.6	17.8	18.0	18.3	6.0	0.64
PM2.5	Spring	AP3	4.9	4.7	0.3	0.7	4.2	14.8	5.4	14.9	0.8	0.63
		AP4	4.8	5.0	-0.1	0.5	-3.5	11.1	-2.9	11.0	0.7	0.72
		AP5	2.9	4.3	-1.4	1.4	-41.3	41.4	-32.6	32.7	1.5	0.43
	Summer	AP3	5.2	5.6	-0.4	0.7	-6.7	11.8	-7.1	12.0	1.0	0.63
		AP4	3.8	7.4	-3.6	3.6	-56.8	56.9	-48.5	48.6	4.8	0.33
		AP5	4.0	9.1	-5.1	5.1	-70.4	70.4	-56.2	56.2	7.1	0.65
	Fall	AP3	8.7	8.2	0.5	2.4	3.5	29.0	6.6	29.2	2.7	0.14
		AP4	7.0	8.2	-1.1	1.4	-11.8	16.0	-13.7	17.0	2.2	0.60
		AP5	8.4	8.6	-0.2	1.4	-8.0	16.6	-2.3	16.2	2.3	0.94
	Winter	AP3	8.7	10.2	-1.5	1.7	-17.1	18.5	-15.0	16.2	2.1	0.71
		AP4	10.1	10.5	-0.4	1.6	-4.3	15.5	-3.5	14.8	1.9	0.66
		AP5	8.1	8.9	-0.8	1.2	-9.3	13.5	-9.1	13.0	1.6	0.65

S-Figure 1. Flowchart of the AIRPACT-5 modeling framework

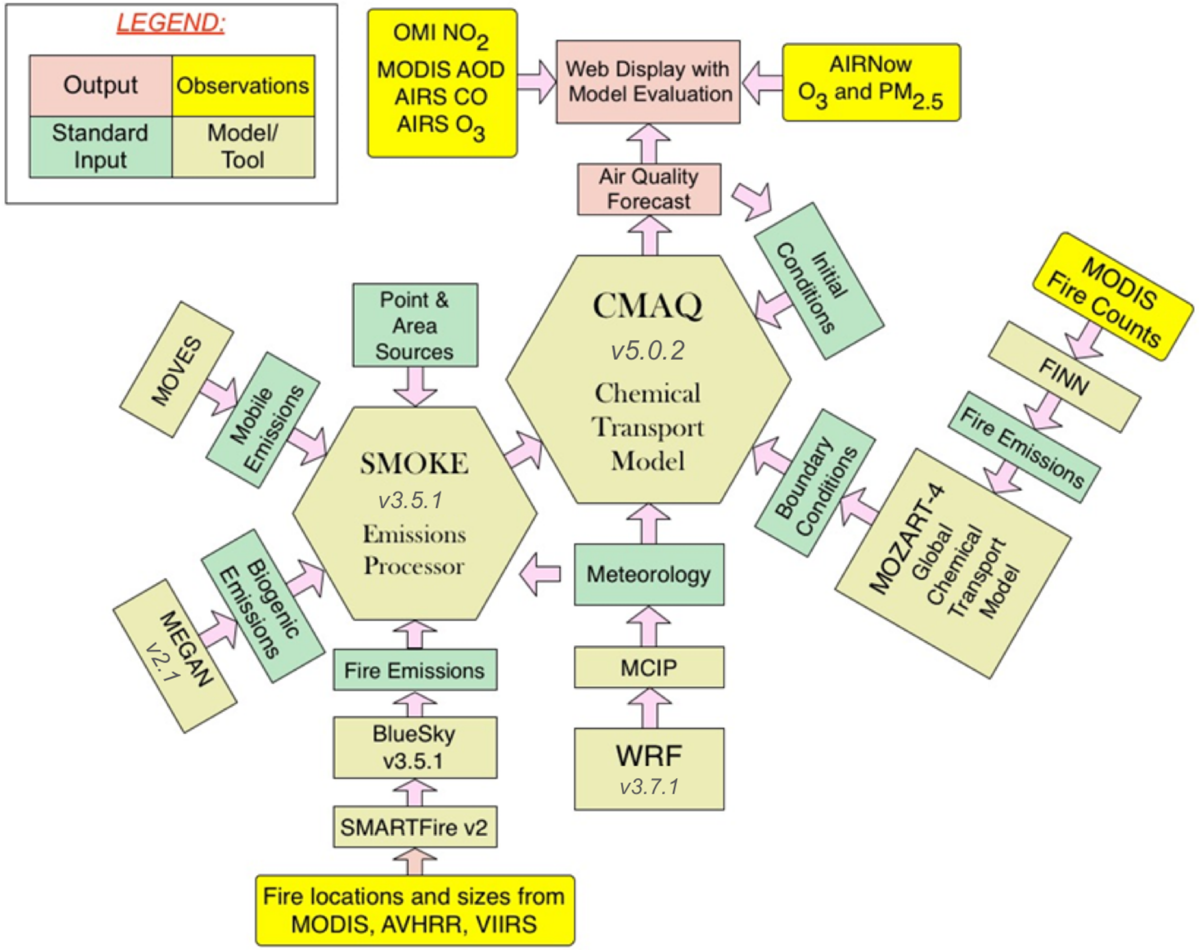

S-Figure 2. Model domain coverage changes from AP-3 to AP-4.

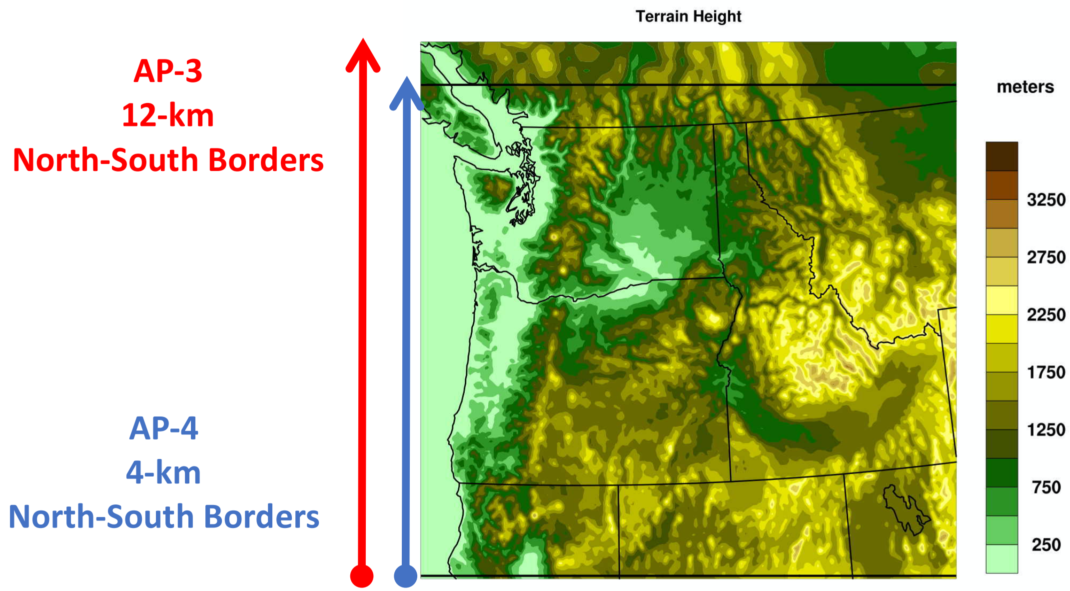

S-Figure 3. Monthly averaged $PM_{2.5}$ at 25 rural sites (a), 34 suburban sites (b), and 30 urban sites (c). The red line denotes AIRPACT forecast, while the black line represents observed AQS data.

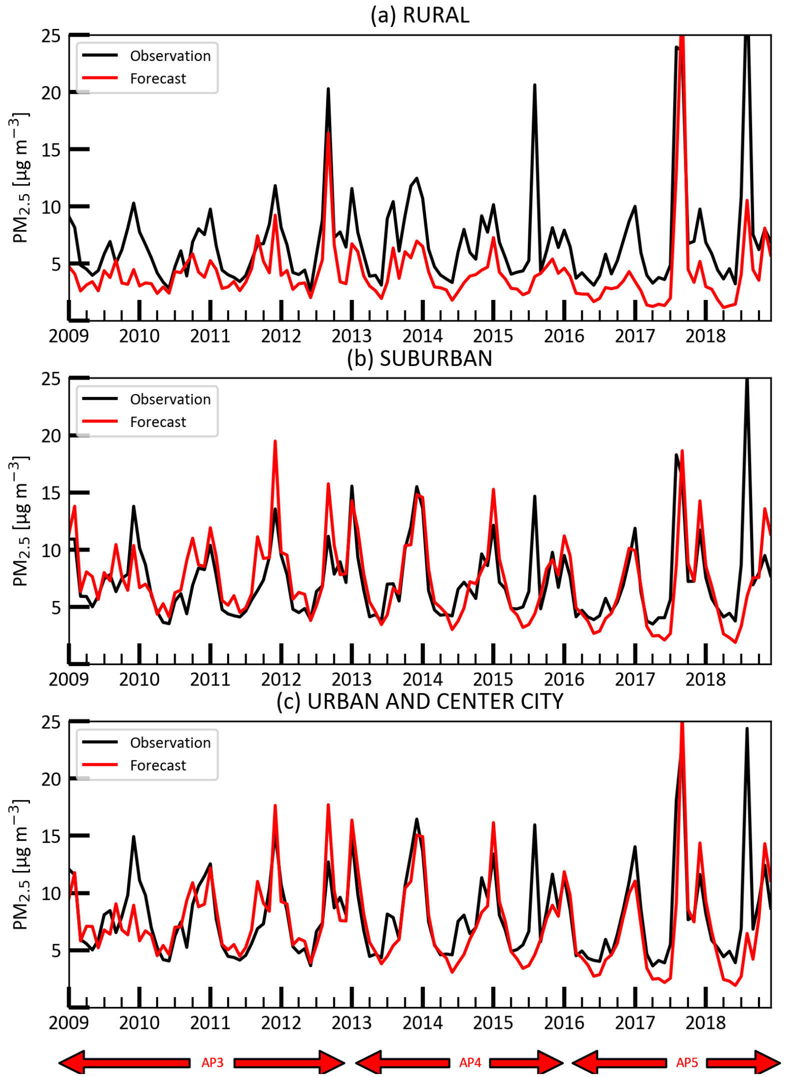

S-Figure 4. Acres of land burned in the PNW within the states of WA (blue), OR (orange), and ID (green). Total acres burned from all three states is denoted in grey.